Sorptive Removal of 4-Aminophenol from Water Using a Polymeric Sorbent

by

Michael Celarek

A thesis

presented to the University of Waterloo

in fulfillment of the

thesis requirement for the degree of

Master of Applied Science

in

Chemical Engineering

Waterloo, Ontario, Canada, 2017

Author’s Declaration

I hereby declare that I am the sole author of this thesis. This is the true copy of the thesis, including any required final revisions, as accepted by my examiners.

I understand that my thesis may be made electronically available to the public.

Abstract

This study deals with isotherm, kinetics and mechanistic studies pertaining to the sorption of 4-aminophenol from water using poly(ether-block-amide) (PEBA). A combined Langmuir and Freundlich isotherm model is used to fit the sorption isotherm data which forms an S3 type curve. The sorption follows pseudo-second order kinetics and the rate constant was determined using the original as well as the modified pseudo-second order models accounting for the instantaneous solute concentrations during the course of sorption. Diffusion was found to take place during sorption but it works alongside a secondary mechanism once higher concentrations (>100 ppm) are reached. The activation energy for sorption is calculated with both pseudo-second order (52.2 kJ/mol) and internal diffusion (54.0 kJ/mol) models. Presence of electrolytes in the system increases the sorption uptake of 50 ppm 4-aminophenol in PEBA by 20% to 100% at 0.25 wt% to 2.0 wt% NaCl respectively. The PEBA sorbent can be regenerated. Regeneration of the PEBA sorbent is highly effective with water, and even more effective with 99% isopropanol which confirms its reuse.

Acknowledgements

I would like to sincerely thank my supervisor Professor Xianshe Feng for his guidance, assistance and encouragement throughout the two thought provoking years of my master's research and thesis writing. I highly appreciate him taking me under his wing and giving me this incredible academic opportunity at the University of Waterloo.

I would also like to thank my colleagues: Shuishu Lai, Elnaz Halakoo, Boya Zhang, Jiaxin Xu and Waquas Iqbal for their assistance and advice during my studies.

In addition the unwavering support from my parents, brother and girlfriend helped me get through all of the hurdles I faced.

Table of Contents

Author's Declaration ..... **ii**

Abstract ..... **iii**

Acknowledgements ..... **iv**

List of Figures ..... **vii**

List of Tables ..... **x**

List of Symbols ..... **xi**

Chapter 1 ..... **1**

Introduction **1**
1.1 Background 1
1.2 Objectives 2
1.3 Thesis Outline 3

Chapter 2 ..... **5**

Literature Review **5**
2.1 Sorption of Phenolic Compounds 6
2.2 Poly(ether-block-amide) Copolymer for Sorption 8
2.3 Sorption Isotherm Models 11
2.3.1 Sorption equilibrium uptake *12*
2.3.2 Linear isotherm model *13*
2.3.3 Langmuir isotherm model *13*
2.3.4 Freundlich isotherm model *15*
2.4 Kinetic Models 16
2.4.1 Sorption uptake at time t *17*
2.4.2 Pseudo-first order kinetics model *17*
2.4.3 Pseudo-second order kinetics model *18*
2.4.4 Intra-particle diffusion kinetics model *19*

Chapter 3 ..... **21**

Experimental **21**
3.1 Materials 21
3.2 Sorbent Preparation 21
3.3 4-Aminophenol Stability 22
3.4 Sorption Isotherm Studies 24
3.5 Sorption Kinetics Studies 25
3.6 Activation Energy 25

3.7 Effect of NaCl 26
3.8 PEBA Sorbent Regeneration 27
Chapter 4 28

Results and Discussion 28
4.1 Sorption Isotherm Modelling 28
4.2 Sorption Kinetics at Different Initial Concentration 32
4.3 Surface Adsorption or Bulk Sorption 44
4.4 Activation Energy 49
4.5 Effect of NaCl on Sorption 54
4.6 PEBA Sorbent Regeneration 61
Chapter 5 63

Conclusion and Recommendations 63
5.1 Conclusions 63
5.2 Recommendations 64
References 65

Appendix 71

Appendix I – Supporting Figures 71

List of Figures

Fig. 1 Outline of thesis..... 4

Fig. 2 Gas phase sorbate from bulk interacting with available surface sites on sorbent material. Zoomed in section shows the interfacial layer [8]. 6

Fig. 3 Multilayer formation of sorbate on surface of sorbent [8]. 7

Fig. 4 PEBA copolymer where PA represents polyamide and PE represents polyether [24]. 9

Fig. 5 UV/Vis absorption spectrum for 50 ppm 4-aminophenol solution at 295 K over time span of 0 – 44 hours. 23

Fig. 6 Sorption isotherms of 4-aminophenol in PEBA at 293 – 313 K. Symbols: experimental data, solid lines represent model fitting based on a combined Langmuir and Freundlich model. 28

Fig. 7 Langmuir model fitting of 4-aminophenol sorption on PEBA..... 29

Fig. 8 Freundlich model fitting of 4-aminophenol sorption on PEBA. 30

Fig. 9 Experimental data for the sorption of 4-aminophenol at different initial concentrations at 293 K. Solid lines represent pseudo-second order model fit. 33

Fig. 10 Linearized pseudo-first order model for 4-aminophenol sorption on PEBA at different initial concentrations. 34

Fig. 11 Linearized pseudo-second order model for 4-aminophenol sorption on PEBA at different initial concentrations. 34

Fig. 12 Second order rate constant K_2 and its corresponding power fit line versus initial 4-aminophenol concentration alongside K_2 values predicted by the Azizian derived model. 38

Fig. 13 Modified pseudo-second order model predicted uptake against experimental uptake at different 4-aminophenol concentrations. 40

Fig. 14 Data fit to the intra-particle diffusion model for sorption of 4-aminophenol on PEBA at different initial 4-aminophenol concentrations. 42

Fig. 15 Fractional sorption uptake versus $t^{1/2}$ for 4-aminophenol sorption on PEBA at different initial 4-aminophenol concentrations. 43

Fig. 16 Uptake of 4-aminophenol on 0.778 g PEBA sorbent films with different surface areas. 45

Fig. 17 Linearized pseudo-second order model for data from **Fig. 16**. 45

Fig. 18 Sorption of 4-aminophenol in PEBA with and without slicing the PEBA sorbent films (mass 0.771 g and thickness 127 μm) into evenly sized pieces. 47

Fig. 20 Uptake of 4-aminophenol on 56.75 cm^2 PEBA sorbent with different thicknesses..... 48

Fig. 21 4-aminophenol uptake at 50 ppm on PEBA with sorption times at various temperatures 49

Fig. 22 t/Q_t versus time for 4-aminophenol sorption in PEBA at various temperatures. 51

Fig. 23 Q_t/Q_e for 4-aminophenol sorption in PEBA at various temperatures..... 52

Fig. 24 K_2 versus 1/T for 4-aminophenol sorption in PEBA. 52

Fig. 25 D_c versus 1/T for 4-aminophenol sorption in PEBA. 53

Fig. 26 4-aminophenol uptake on PEBA in the presence of different concentrations of NaCl at 293 K. Control designates 0% NaCl content. Initial concentration of aminophenol 50 ppm..... 54

Fig. 27 4-aminophenol uptake over time on PEBA in the presence of different concentrations of NaCl at 293 K. Control designates 0% NaCl content. Initial concentration of aminophenol 500 ppm. 55

Fig. 28 t/Q_t versus time for sorption of 4-aminophenol (initial concentration 50 ppm) on PEBA in the presence of different concentrations of NaCl. 57

Fig. 29 Q_t/Q_e versus $time^{1/2}$ for sorption of 4-aminophenol (initial concentration 50 ppm) on PEBA in the presence of different concentrations of NaCl. 57

Fig. 30 t/Q_t versus time for sorption of 4-aminophenol (initial concentration 500) ppm on PEBA in the presence of different concentrations of NaCl. 58

Fig. 31 Q_t/Q_e vs $time^{1/2}$ for sorption of 4-aminophenol (initial concentration500 ppm) on PEBA in the presence of different concentrations of NaCl. 58

Fig. 32 Second order rate constant (K_2) of 4-aminophenol solutions at 50 and 500 ppm on PEBA versus different NaCl concentrations. 60

Fig. 33 Diffusion coefficient (D_c) of 4-aminophenol solutions at 50 and 500 ppm on PEBA versus different NaCl concentrations 60

Fig. 34 Desorption of 4-aminophenol in PEBA using water and isopropanol after consecutive sorption/desorption runs 62

List of Tables

Table 1 Composition of PEBA according to grade and commercial source. 10

Table 2 Measurable oxidation of aqueous 4-aminophenol at 50 ppm according to UV-Vis absorption data at 296 nm. 24

Table 3 Langmuir and Freundlich combined model fitting parameters and statistical analysis for 4-aminophenol on PEBA sorbent. 31

Table 4 Parameters for kinetic sorption models. 35

Table 5 Rate constant determined from modified pseudo-second order kinetic sorption model. 40

Table 6 Parameters for diffusion models of different initial concentrations of 4-aminophenol on PEBA sorbent. 44

Table 7 Sorption kinetic parameters based on pseudo-second order and intra-particle diffusion models for sorbent films with different surface areas and the same masses (0.777 g). 46

Table 8 Activation energy for pseudo-second order rate constant and intra-particle diffusivity for sorption of 4-aminophenol on PEBA as temperature changes. 54

Table 9 Pseudo-second order rate constants and intra-particle diffusivities for sorption of 4-aminophenol at 50 ppm and 500 ppm on PEBA as NaCl concentration changes. 61

List of Symbols

Q_e	Equilibrium sorption uptake (mmol/g)
V	Volume of solution (mL)
C_o	Initial solution concentration (mmol/mL)
C_e	Sorption equilibrium solution concentration (mmol/mL)
M	Mass of PEBA sorbent (g)
t	Time (min)
Q_t	Sorption uptake at time t (mmol/g)
C_t	Solution concentration at time t (mmol/L)
Q_m	Maximum sorption capacity (mmol/g)
K_L	Langmuir constant (mL/mmol)
K_F	Freundlich constant (dimensions are based on n)
n	Factor for system curvature
K_1	First order rate constant (min^{-1})
K_2	Second order rate constant (g/mmol·min)
K_2'	Modified second order rate constant (g/mmol·min)
k_i	Intra-particle diffusion constant ($mmol \cdot g^{-1} \cdot min^{-1/2}$)
C	Intensity of the boundary layer effect (mmol/g)
l	Thickness of the sorbent material (m)
K	True equilibrium rate constant (mL/mmol)
k_a	Sorption rate constant (mL/mmol·min)

k_d	Desorption rate constant (min^{-1})
SA	Surface area (cm^2)
A	Temperature independent pre-exponential factor
R	Universal gas constant (kJ/mol·K)
T	Temperature (K)
E_a	Activation energy (kJ/mol)
D_o	Temperature independent pre-exponential factor
D_c	Intraparticle diffusivity (m^2/min)

Chapter 1

Introduction

1.1 Background

Phenols are important chemical compounds used in many industrial applications ranging from pesticides to pharmaceuticals. Industries either consume or synthesize these phenol compounds, producing waste process streams. Phenol contaminants make their way into process water and must be removed before the water can be reused or discharged. Their removal is important since they are toxic, corrosive and can accumulate in the environment doing further damage to natural habitats [1].

Nearly all of acetaminophen production in the world follows one of four routes: phenol, 4-nitrochlorobenzene, nitrobenzene or p-hydroxyacetophenone hydrazine, all of which use a highly genotoxic intermediate molecule called 4-aminophenol [2][3]. This compound can make its way into wastewater streams and expose high risk for environmental pollution [4]. The method used for the treatment of the water streams containing 4-aminophenol certainly depends on the production process used. In general, processes frequently proposed to remove phenols from water include: coagulation, sedimentation, chemical oxidation, filtration, ion exchange and reverse osmosis [5]. Another option commonly used is adsorption, which is widely used in removal of organic and inorganic micropollutants from aqueous streams [5]. The most common adsorbent used for adsorptive removal is activated carbon, but the cost associated with its regeneration, including the brittleness it exhibits (causing it to form fine carbon particulates,

which are lost during use) calls for finding an alternative sorbent material [4]. Poly(ether-block-amide) copolymer (PEBA) shows high selectivity for various phenols and cyclic compounds in pervaporation studies [1,6]. PEBA contains both electron withdrawing groups (amide and ester) and electron donating groups (ether) while 4-aminophenol contains electron donating groups (phenol and amine), stressing potential interactions between these compounds. This means PEBA is likely to be suitable for removal of 4-aminophenol from water through sorptive means.

This work is aimed at sorption of 4-aminophenol from water using PEBA 2533, focussing on sorption isotherm, kinetics and interpretive system modelling. They offer understanding for the mechanisms involved and further interactions with compounds such as NaCl, which can help predict sorptive behaviour of the system when exposed to electrolytes.

As a notice in this study, the term “sorption” was used throughout to describe the overall mechanism for 4-aminophenol interacting with PEBA as opposed to “adsorption” which is a surface phenomenon. As shown later in this study, 4-aminophenol did not only interact with the external surface of the PEBA but also diffused into the interior, indicating that “sorption” was a better representative term for this system.

1.2 Objectives

This study focused on treating 4-aminophenol, a contaminant found in wastewater, through a sorption method. The experiments involved include:

(1) Investigating the sorptive effectiveness of PEBA sorbent for removal of 4-aminophenol at different operating conditions (temperature, initial concentration)

(2) Determining parameters and relationships to understand the mechanisms of sorption

(3) Studying the effects of an additional impurity in the system (NaCl) on the sorption performance, and also the regeneration and reuse of the PEBA sorbent

1.3 Thesis Outline

This study is composed of five chapters, which have been organized as shown in **Fig. 1.**

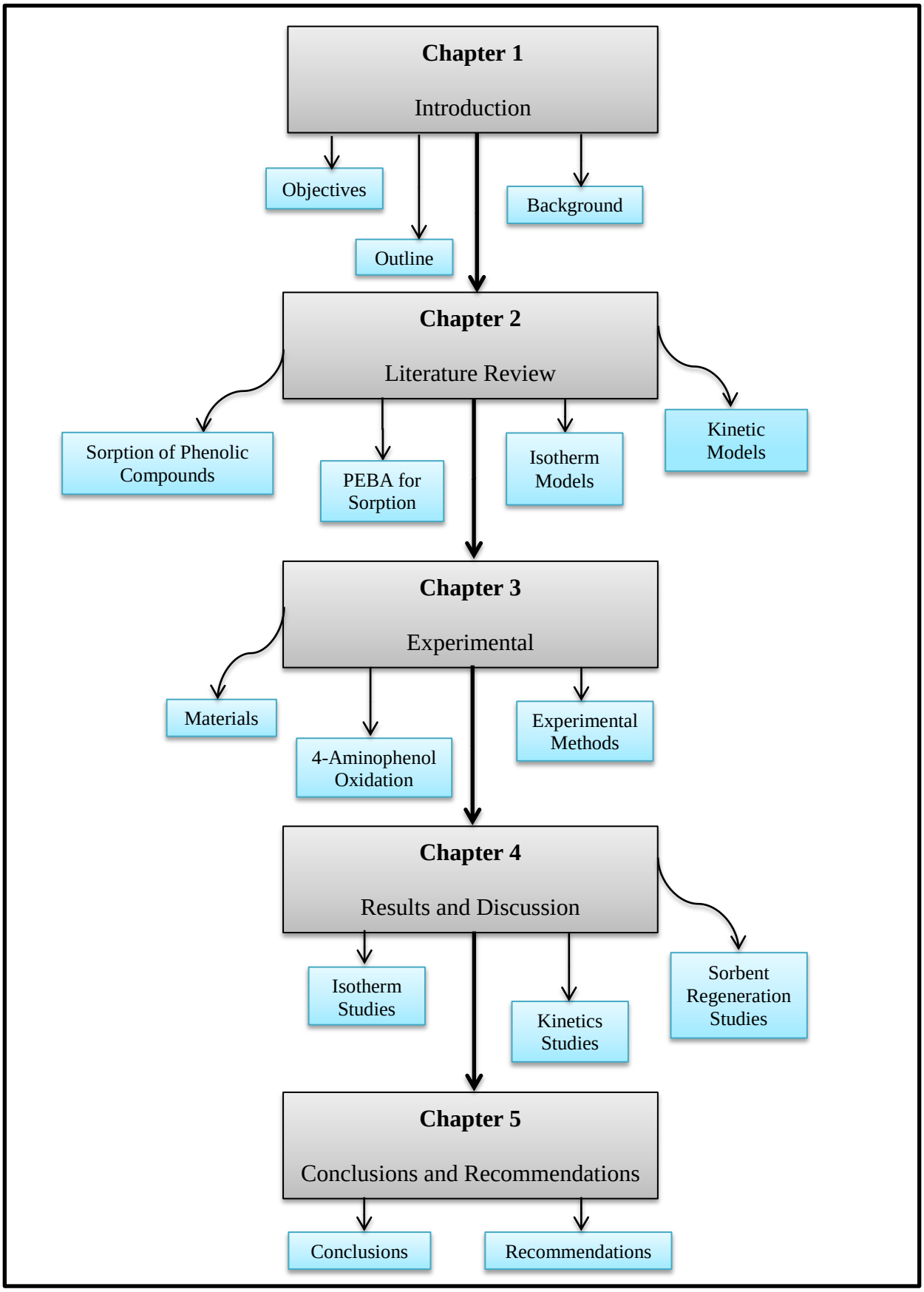

Fig. 1 Outline of thesis.

Chapter 2

Literature Review

Sorption is a broad topic which can be broken down for study in a number of ways. The topics focused on in this review include: removing phenolic compounds from water with sorption, poly(ether-block-amide) copolymer (PEBA) as a sorbent, and modelling sorption isotherms and kinetics.

As mentioned previously, phenolic compounds are critical albeit toxic chemicals which, depending on industry, have an importance in their removal from wastewater. Many past studies have approached chemical separation using sorption, and different sorbent compounds have had their effectiveness compared with one another. PEBA showed unique selectivity to phenols in pervaporation processes, and thus its effectiveness as a sorbent is of interest. Finally, the mathematical basis to describe the act of sorption concerning both isotherms and kinetics is critical to a deep understanding on the mechanisms involved. As such, common corresponding models will be investigated while further modifications to some of these models will also be reviewed.

2.1 Sorption of Phenolic Compounds

The process of sorption can fall under one of four major scenarios depending on which phases are in the system: liquid-liquid, liquid-gas, solid-liquid or solid-gas. Regardless of the phases in contact, the general mechanism of sorption is the same; a physical, chemical or biological process causing molecules to accumulate in the interfacial layer. More specifically, sorption is the change in concentration of these molecules at the interface in relation to the bulk of the other phase(s) [7]. This gathering of material at the interfacial layer is illustrated in **Fig. 2**.

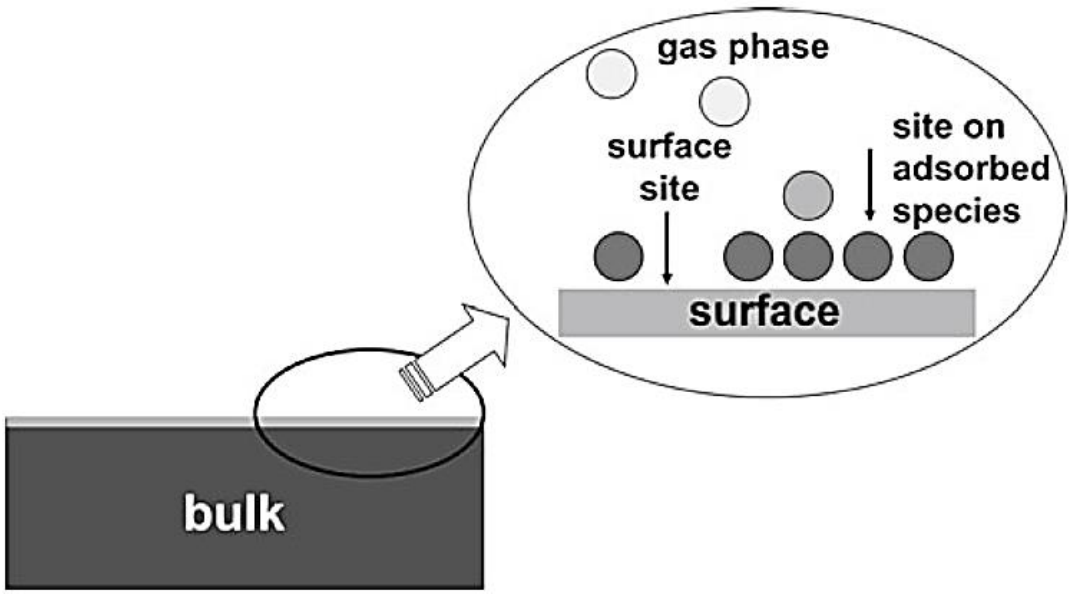

Fig. 2 Gas phase sorbate from bulk interacting with available surface sites on sorbent material. Zoomed in section shows the interfacial layer [8].

Depending on the sorbate/sorbent system, the accumulation of sorbate on the sorbent can be a single molecular layer (monolayer) or if interactions between the sorbate permit, multiple layers can gather on the sorbent (multilayer). This is illustrated in **Fig. 3**.

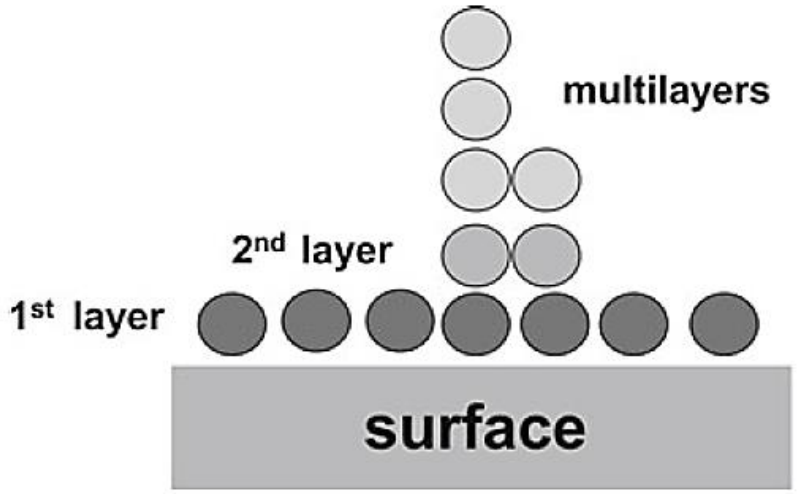

Fig. 3 Multilayer formation of sorbate on surface of sorbent [8].

In essence, the overall interactions between the sorbent and sorbate in combination with the sorbate and other sorbate molecules is what determines the effectiveness of a sorption-based separation. These sorts of interactions can be predicted using isotherm and kinetic sorption models but will be discussed in a later section.

There is a wide application of sorption for separation and purification, such as manufacturing industries, chemical industries and wastewater treatment. There are many sorbents applied towards the removal of different sorbates. For removing phenols, some highly studied sorbents include activated carbon, mineral based sorbents, and polymeric based sorbents.

Activated carbon is a widely recognized sorbent used to remove many different pollutants. Some of its characteristics, including well-defined microporosity, presence of functional groups and high potential for modification, give it great sorption potential for phenols [9]. The high porosity of activated carbon means its effective surface area is large, ranging from 600 – 2000 m^2/g [10]. Primarily, the chemical composition of activated carbon is what determines its sorptive effectiveness, particularly the presence of oxygen and hydrogen on

surface groups [9]. One drawback for activated carbon is that its production is not environmentally friendly, with abundant research going into finding alternative low-cost carbon sources [11].

Mineral based sorbents comprise many materials including clay, zeolite and siliceous minerals. Clay materials, such as bentonites, kaolinite and diatomite are attractive sorbents since they are cheap to produce, plentiful and can also be chemically modified in order to improve their properties [12,13]. Studies have shown their effectiveness in removing phenols from water [14,15,16] but their main drawback is their poor sorption capacity. Zeolites are similar to clay materials, and they are classified as low-cost sorbents which are also widely available [17]. Their sorption of phenols seems to have been studied extensively, with a number of investigations turning up positive results in this application [18,19,20]. Unfortunately, their sorption capacity is even lower than that of clay materials. Siliceous minerals (i.e., materials that contain silica, SiO_2) can overlap in classification with other mineral based sorbents. For example, montmotillonites contain silica but are also a clay material. They have shown a good affinity for phenols and chlorinated phenols after modifications with tetramethylammonium (TMA) chloride and tetramethylphosphonium (TMP) bromide according to a study performed by Lawrencea et al [21]. Further studies on sorption of phenols with siliceous minerals need to be performed.

2.2 Poly(ether-block-amide) Copolymer for Sorption

Poly(ether-block-amide) copolymer (PEBA) is a thermoplastic elastomer which consists of ether blocks and amide blocks covalently bonded together with amide linkages. The polyamide sections are hard blocks and give the material its strength, while the polyether

sections are soft blocks giving the material its flexibility and elasticity [22]. Advantageous properties of PEBA include it being lightweight, resistant to impact and shock, transparent, high chemical resistance and easy to shape and extrude [23]. A molecular representation of PEBA is shown in **Fig. 4**.

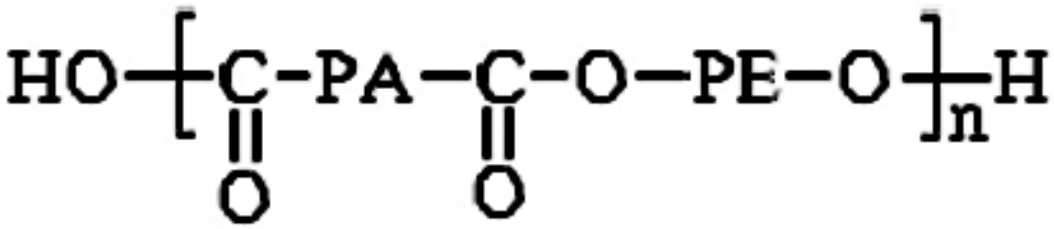

Fig. 4 PEBA copolymer where PA represents polyamide and PE represents polyether [24].

PEBA with sufficiently high molecular weight was first synthesized and studied in the 1980s [22,25,26] and commercially available under the trade name of PEBAX® by Atochem [24]. Since its inception, PEBA has been synthesized using various polyamides (polyamide-11, polyamide-12, polyamide-6) and polyethers (polyoxytetramethylene, polyoxyethlene, polyoxypropylene), giving the resulting PEBA material different properties [22]. Furthermore, different ratios of each polyamide and polyether segments form different grades of PEBA as characterized in the following table.

Table 1 Composition of PEBA according to grade and commercial source.

PEBA Grade	Source of PEBA	Composition				Ref.
		Polyether		Polyamide		
1074	Arkema Inc.	55	wt %	45	wt %	[27]
1657		60		40		
2533		80		20		
3533	AtoChem Inc	75	wt %	21	wt %	[28]
4033		52		43		
P2533	Atofina Chemicals	84.68	mol %	11.92	mol %	[24]
P3533		83.61		13.00		
P4066		70.41		27.15		
P6333		36.96		60.47		
P7033		24.78		72.95		
2533	Arkema Inc.	86	mol %	14	mol %	[29]
3533		75		25		
4033		71		29		
5533		47		53		
6333		37		43		
7033		25		75		
7233		20		80		

The different PEBA grades have a four number naming scheme where the first two numbers signify the shore D hardness (10, 16, 25, 35, 40, 55, 63, 70, 72) [29]. **Table 1** shows that as the polyamide content in PEBA increases, so does the hardness of the PEBA copolymer. This is supported by previous points made that the polyamide sections give the material its strength and rigidity.

An important consideration for an effective sorbent material is its porosity. Fortunately for PEBA, the soft polyether content gives it the necessary amorphous property to allow for easy diffusion. With this in mind, the PEBA grade with high polyether content is more suitable for sorption purposes. Therefore, PEBA 2533 (80 – 86 % polyether) appears to be appropriate, which is further supported by its affinity to various compounds shown in gas permeation studies [30], pervaporation studies [1,31,32] and sorption studies [1].

2.3 Sorption Isotherm Models

As sorption process proceeds with time, the concentrations of sorbate in the bulk solution and on the surface of the sorbent (in the interior of the sorbent if interior diffusion occurs) will change accordingly. This can be represented and predicted using mathematical models for sorption isotherms that correlate the sorption uptake in the sorbent at equilibrium versus solute concentration in the bulk phase at a given temperature.

Sorption isotherms are considered the most important fundamental study which can be performed to sense how effective the sorbent is in terms of its affinity to the sorbate [33]. Now, depending on the phases of the system, the actual method for characterizing the capacity of the sorbent and amount of sorbate in the bulk is different. For example, if the bulk solution is in the gas phase, partial pressure is used; if it is in the liquid phase, then molar concentration may be used conveniently. This study deals with sorption of solute from the liquid phase. Sorbent sorption capacity at equilibrium can be characterized by the sorbate sorbed per unit mass of sorbent based on the following:

$$Q_e = f(C_e, T) \quad \textbf{(1)}$$

where Qe is usually expressed in terms of moles of sorbate per gram of sorbent, and C_e is molar concentration of solute in the bulk liquid.

The most common isotherm models discussed in literature include the Linear model, Langmuir model and Freundlich model. Each of these isotherm models applies to representing a different sorption mechanism occurring at the molecular level. Determining which model is best for a particular system, by obtaining model parameters, can best be done by analyzing the experimental data of sorption uptake at different sorbate concentrations in the solute solution at given temperatures.

2.3.1 Sorption equilibrium uptake

The first step in determining an isotherm model requires the determination of sorption uptake at equilibrium. Since an infinite amount of time is required to reach true equilibrium, the point at which sorption slows down to a perceived stop (in regards to the apparatus used to measure concentration) is an appropriate point to call equilibrium.

Equilibrium sorption uptake, Q_e (mmol/g), can be calculated with Eq. (2).

$$Q_e = \frac{V \cdot (C_0 - C_e)}{M} \quad \textbf{(2)}$$

where V (mL) is volume of solution, C_o (mmol/mL) and C_e (mmol/mL) are initial and equilibrium solution concentrations, respectively, and M (g) is mass of sorbent. Eq. **(2)** can be implemented in each of the isotherm models mentioned previously to determine model parameters.

2.3.2 Linear isotherm model

The linear isotherm model is the simplest containing only a single model parameter. It is analogous to Henry's law and can be represented by Eq. **(3)** [34]

$$Q_e = K_H \cdot C_e \quad \textbf{(3)}$$

where Q_e (mmol/g) is the sorption amount at equilibrium and K_H (mL/g) is Henry's sorption constant. The primary use for the linear isotherm model is that it can be applied to the initial period of many sorption systems (i.e., when C_e is sufficiently low).

2.3.3 Langmuir isotherm model

The Langmuir model is one of the most widely applied isotherm models used to describe various sorption systems. It is derived from the equilibrium between free sorbate molecules/vacant sites on the sorbent material and occupied sites on the sorbent material. This means there must be two rate constants in play: K_a being the adsorption rate constant and K_d being the desorption rate constant [35]. The sorption equilibrium can be visualized in the following way:

$$A + B \underset{K_a}{\Rightarrow} AB \quad \textbf{(4)}$$

and

$$A + B \underset{K_d}{\Leftarrow} AB \quad \textbf{(5)}$$

where A is the free sorbate molecule, B are vacant sorption sites on the sorbent material, and AB represents the occupied sites on the sorbent material.

The Langmuir isotherm can be represented by Eq. (6) [35]:

$$Q_e = \frac{Q_m \cdot K_L \cdot C_e}{1 + K_L \cdot C_e} \quad \textbf{(6)}$$

where Q_m (mmol/g) is the maximum sorption capacity, and K_L (mL/mmol) is the Langmuir constant. Eq. (6) can be linearized for model fitting in the following form:

$$\frac{1}{Q_e} = \frac{1}{Q_m \cdot K_L}\frac{1}{C_e} + \frac{1}{Q_m} \quad \textbf{(7)}$$

Plotting Q_e^{-1} versus C_e^{-1} gives a straight line that can be used to determine model parameter Q_m from the y-intercept and K_L from the slope.

The Langmuir sorption theory is based on assumptions of monolayer sorption, uniform sorption across the surface, finite sorption sites and no interactions between lateral sorbed molecules [36]. This means that once the sorption sites have been entirely filled, sorption ceases due to saturation of the sorption sites.

Since the Langmuir constant has a clear physical meaning, some studies have used it for the calculation of the equilibrium constant K_o towards the determination of the Gibbs energy change of sorption, ΔG^o:

$$\Delta G^o = -RT \ln K_o \quad \textbf{(8)}$$

where R (kJ/mol·K) is the universal gas constant and T (K) is the temperature. Even though some studies directly interchange K_L and K_o with one another [17,37], this is strictly speaking incorrect practice. K_o is dimensionless, but K_L has the dimensions of volume per mol. One attempt was to convert K_L to K_o according to a few studies performed by Milonjic and Zhu et al by multiplying a property of the sorbate solution (i.e., the molar density of water, which units are equivalent to units of concentration) to make it dimensionless [38,39]. The problem with such treatment is that since the activity of a solution is the ratio of its own concentration to the concentration of a standard reference solution, the ratio Milonjic and Zhu et al used to convert K_L effectively perform the same task, and the units will always cancel out [40]. In essence, this newly formed dimensionless term is not particularly meaningful and clear.

2.3.4 Freundlich isotherm model

Another commonly used isotherm model is the Freundlich model, which is based on semi-empirical formulation of the sorption uptake that results from both multilayer sorption and heterogeneous sorption over its layers [41].

The Freundlich isotherm can be represented by Eq. (9) [41]:

$$Q_e = K_F \cdot C_e^{\frac{1}{n}} \quad \textbf{(9)}$$

where K_F (dimensions are based on the value of n) is the Freundlich constant and n is a factor for system curvature. Eq. (9) can be linearized for model fitting in the following form:

$$\ln Q_e = \ln K_F + \frac{1}{n} \ln C_e \quad \textbf{(10)}$$

where Q_e versus C_e was plotted on logarithmic scale to determine model parameters: n from the slope and K_F from the y-intercept.

The n term in this model is indicative of the intensity of sorption, while $1/n$ is considered as a heterogeneity factor. Unlike the Langmuir constant, the Freundlich constant has no clear physical meaning and thus it is inherently inappropriate to use this term to derive the equilibrium constant K_o. Some studies have proposed transforming K_F into K_o according to the density of the solvent of the bulk solution [38] but since the units of K_F are influenced by the value of n, this fix is only possible if $n = 1$.

2.4 Kinetic Models

Following a sorption rate from as soon as the sorbent comes into contact with the sorbate (at $t = 0$) to any other point during sorption (at $t = t$) can be described as the sorption kinetics. The sorption data has been represented most commonly with one of two major sorption models: pseudo-first order model and pseudo-second order model. These models assume the sorption rate

is controlled by the liquid/solid interface [42]. On the other hand, if the sorption process is controlled by diffusion, the intra-particle diffusion model may be implemented.

2.4.1 Sorption uptake at time t

In order to determine the kinetic parameter in a kinetic model, the sorbate uptake at time *t* is required. This uptake, Q_t (mmol/g), can be determined with Eq. **(11)**

$$Q_t = \frac{V \cdot (C_0 - C_t)}{M} \quad \textbf{(11)}$$

where C_t (mmol/L) is solute concentration in the solution at time *t* (min).

2.4.2 Pseudo-first order kinetics model

Lagergren proposed the pseudo-first order kinetics model in 1898 which since then has been used in many studies to describe sorption processes [43]. The pseudo-first order kinetics model can be represented by Eq. (12):

$$\frac{dQ_t}{dt} = K_1(Q_e - Q_t) \quad \textbf{(12)}$$

where K_1 is the first order rate constant. Eq. (12) can then be integrated between the limits of Qt = 0 at $t = 0$ and $Q_t = Q_t$ at $t = t$, and rearranged into the following linear form:

$$\ln(Q_e - Q_t) = -k_1 t + \ln Q_e \quad \textbf{(13)}$$

where ln(Q_e – Q_t) versus t can be plotted to determine model parameters: k_1 from the slope and Q_e from the y-intercept.

The pseudo-first order kinetics model assumes that the sorption rate is proportional to sorption capacity available at that time and thus the sorption rate is primarily based on (Qe -Qt) and not explicitly on the bulk solute concentration in the solution [44].

2.4.3 Pseudo-second order kinetics model

The pseudo-second order kinetics model was proposed in the 1980's paved with studies of Blanchard et al. and Gosset et al., far later than the introduction of the pseudo-first order kinetics model [45,46]. The popularity of the pseudo-second order kinetics model reached greater heights after Ho and McKay analyzed over 70 studies and concluded that the pseudo-second order model represented the data superbly well in comparison with the pseudo-first order model [47].

The pseudo-second order kinetics model can be represented by Eq. (14) [48]:

$$\frac{dQ_t}{dt} = K_2(Q_e - Q_t)^2 \quad \textbf{(14)}$$

where K_2 is the second order rate constant. Eq. (14) can then be integrated between the limits of Qt = 0 at t = 0 and Q_t = Q_t at t = t, and rearranged into the following linear form:

$$\frac{t}{Q_t} = \frac{1}{k_2 Q_e^2} + \frac{1}{Q_e} t \quad \textbf{(15)}$$

where ${}^{t}/_{Qt}$ versus t can be plotted to determine model parameters: Q_e from the slope and k_2 from the y-intercept.

The rate limiting step for the pseudo-second order model is chemical sorption with exchange and sharing of electrons between the sorbent and sorbate. Similar to the first order model, the sorption rate for this model is also primarily based on the sorption capacity of the sorbent available at that time and not explicitly on solute concentration in the bulk solution [44].

2.4.4 Intra-particle diffusion kinetics model

The intra-particle diffusion model was first proposed in 1962 by Weber and Morris with a focus originally on the sorption of biologically-resistant pollutants in wastewater [49,50]. They discovered that solute uptake was proportional to $\sqrt{t}$ in the initial stage of sorption, leading to the linear form of the intra-particle diffusion model. It can be represented by Eq. (16):

$$Q_t = k_i\sqrt{t} + C \qquad \textbf{(16)}$$

where k_i (mmol·g^{-1}·min$^{-1/2}$) is the intra-particle diffusion constant and C (mmol/g) represents the intensity of the boundary layer effect. A plot of Q_t versus $\sqrt{t}$ could be used to determine the model parameters: k_i from the slope and C from the y-intercept.

If the Q_t versus $\sqrt{t}$ plots as suggested by Eq. (16) are linear, then the intra-particle diffusion is likely a dominant factor in the system, but if the straight line doesn't pass through the origin (i.e., $C \neq 0$), then the sorption might be controlled by intra-particle diffusion in combination with boundary layer effects. If the data passes through the origin, then the intra-

particle diffusion is dominating over the boundary layer effect in the sorption rate controlling steps.

Taking the intra-particle diffusion model further, it is possible to use the slope of a straight line representing the fractional uptake ($^{Qt}/_{Qe}$) versus $\sqrt{t}$ to calculate the intra-particle diffusivity (D_c) according to Eq. (17) [51]:

$$\frac{Q_t}{Q_e} \approx \frac{4}{l}\left(\frac{D_c t}{\pi}\right)^{\frac{1}{2}} \quad \textbf{(17)}$$

where l (m) designates the thickness of a homogeneous sorbent material in planar geometry (e.g., flat films or membranes). Eq. (17) is only appropriate to use if the sorption time is relatively short and when only considering the initial stage of sorption (ie. $^{Qt}/_{Qe} < 0.5$) [52]. This is because at that time the boundary layer effect is not as significant [51].

Chapter 3

Experimental

3.1 Materials

PEBAX 2533 SA01 (Arkema), 4-aminophenol (99%, Sigma-Aldrich), N,N-dimethylacetamide (99%, Sigma-Aldrich), 2-propanol (99%, Delon Laboratories) and NaCl (99%, EMD Millipore) were purchased from commercial suppliers and used as received. N_2 and deionized water were supplied by University of Waterloo. Stock solutions of 4-aminophenol were prepared by dissolving known quantities of 4-aminophenol in deionized water. Dilutions of this stock solution were then used for formation of standard solutions.

The lab equipment used included: Shimadzu UV mini 1240 UV-Vis spectrophotometer, Starrett micrometer, Cole-Parmer Polystat 12101-31 temperature controller, Precision Scientific Thelco Model 16 heater, Mettler Toledo PM200 scale, Corning PC-520 hot plate.

3.2 Sorbent Preparation

Sorbent material was prepared by mixing PEBAX 2533 with N, N - dimethylacetamide (DMAc) to form a 15 wt% solution. The solution was vigorously stirred for 3 hours in a water bath at a constant temperature of 353 K. The solution was sealed and left to rest for 24 hours in a heater at 343 K to remove entrapped air bubbles. Volume of solution was measured out using 20 mL syringes and dispensed into petri dishes which were preheated to 343 K. Preheating ensured the solution did not cool down before it completely evaporated. The petri dishes were then left in

a heater at 343 K for 24 hours to evaporate the DMAc solvent. The sorbent was peeled off the petri dishes using forceps and washed several times with deionized water to remove residual DMAc. They were then left to dry for 8 hours in a heater at 343 K. The sorbent film/membrane thickness and surface area were measured using a Starrett micrometer and calipers respectively. Sorbent material was stored in Parafilm covered petri dishes to minimize contamination and moisture accumulation.

3.3 4-Aminophenol Stability

Aqueous 4-aminophenol exhibits instability to a certain degree when exposed to oxygen and initially oxidizes to 4-benzoquinone monoamine but eventually oxidizes to NN'-bis-(4-hydroxyphenyl)-2-hydroxy-5-amino-1,4-benzoquinone according to the mechanism proposed by Brown and Corbett [53]. Once measurable oxidation of 4-aminophenol occurs, the colour of its solution begins to change from clear to a brown shade signifying that this degradation process has begun. As the reaction proceeds, the solution turns into a darker brown/black. In order to minimize oxidation, stock 4-aminophenol solutions were constantly contained under N_2 which effectively kept them stable, at least for 7 days over which the experiments were carried out.

It was necessary to determine how long the 4-aminophenol solutions could remain stable once exposed to air since the experiments could not be run under constant N_2 conditions for the entire duration, in particular when removing solution samples to place in the UV-Vis spectrophotometer. In order to determine the stability limit, a UV-Vis absorption spectrum plot using 1cm light path cells between 200 – 700 nm wavelengths were generated every hour until a deviation was noticed.

As can be seen in **Fig. 5**, a deviation at 296 nm and 380 nm was observed after 180 min at 295 K signifying the approximate time at which the oxidation process has noticeably begun.

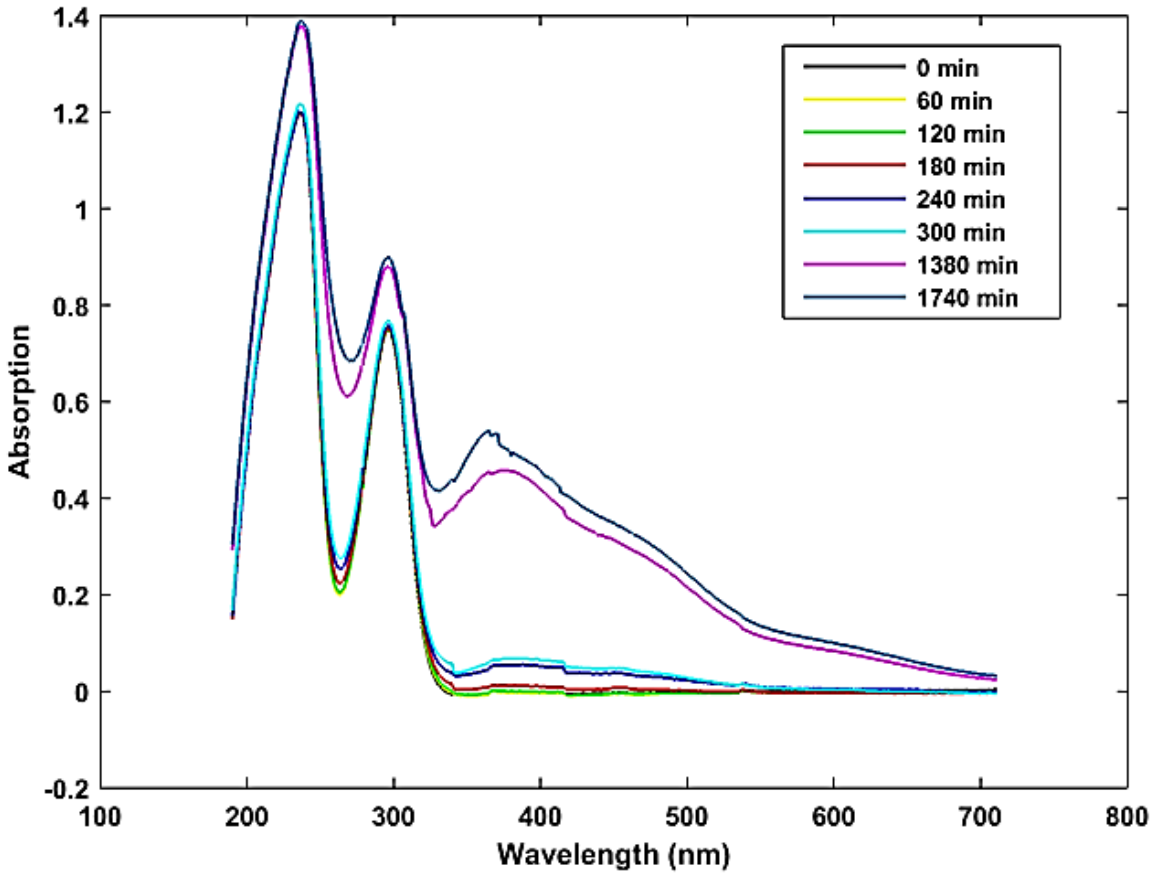

Fig. 5 UV/Vis absorption spectrum for 50 ppm 4-aminophenol solution at 295 K over time span of 0 – 44 hours.

There was a limited time frame after removing 4-aminophenol from the stock solution before the oxidation was noticeable and experiments became unreliable. The same procedure from **Fig. 5** was repeated in a water bath at each temperature used in this study to acquire oxidation time limits (See **Appendix II**). The sorption experiment must attain equilibrium before this time limit is reached to ensure acceptable results. The time limits can be seen below in **Table 2**.

Table 2 Measurable oxidation of aqueous 4-aminophenol at 50 ppm according to UV-Vis absorption data at 296 nm.

Temperature (K)	273	283	293	295	298	303	308	313
Start of oxidation (min)	2000	1140	360	180	180	120	120	45

The speed of oxidation, represented by change in absorption at 296 nm, is higher from 180 – 300 min (Δabs/min = 1.33E-4 min^{-1}) than from 300 – 1380 min (Δabs/min = 1.07E-4 min^{-1}) as shown in **Fig. 5**. This signifies that the oxidation reaction slows down over time (after 180 min) and further supports that the nonexistent change in absorption from 0 – 180 min is a reliable metric for 4-aminophenol stability.

3.4 Sorption Isotherm Studies

Sorption isotherm data was collected using batch sorption experiments with 4-aminophenol solutions in 33 mL bottle capacities. The concentration range was chosen relative to 70% of the maximum solubility of 4-aminophenol at the lowest temperature tested (293 K), which is about 4400 ppm. This resulted in a concentration range from 0 – 3000 ppm (300 ppm steps) at 293 – 313 K with 5 K increments. The sorbent material had a weight of 0.2 ±0.02 g with a thickness of 125 ±10 μm and a surface area of 19 cm^2. The liquid solution was agitated throughout the duration of the sorption process to ensure solution homogeneity while controlling temperature with a water bath.

The sorbent film was immersed in the 4-aminophenol solutions and left in the water bath until equilibrium was reached according to preliminary kinetics tests performed at each temperature. These preliminary kinetics tests reported a minimum length of time required for

submersion (80, 50, 40, 25 and 10 min for 293, 298, 303, 308 and 313 K respectively). They were submerged for at least this length of time, but never longer than the times shown in **Table 2**. Once sorption equilibrium was reached, a small portion of the solutions were diluted for concentration measurements with the UV/Vis-Spectrophotometer at a wavelength of 296 nm.

3.5 Sorption Kinetics Studies

Batch sorption kinetics studies were performed in 100 mL bottles with controlled sorbent properties. Each sample was agitated throughout the duration of the sorption process to ensure solution homogeneity while also controlling temperature with a water bath.

Sorbent films with the same mass (0.778±0.001 g), but different surface areas (77.9, 56.8 and 23.8 cm^2) at a constant temperature (293 K) were used in the sorption kinetics study to get an insight into the mechanisms of sorption. In addition, sorbent films with the same surface area (57 cm^2), but different thicknesses (100±10, 125±10 and 150±10 μm) at a constant temperature (293 K) were used for the same reason. Sorbent films with the same surface area (57 cm^2) and mass (0.55±0.01 g) but different initial solute concentrations at constant temperature (293 K) were used for insight into the sorption kinetics.

The 4-aminophenol concentrations were monitored throughout the sorption process (100 ppm and above were first diluted) and measured with the UV/Vis-Spectrophotometer.

3.6 Activation Energy

Sorbent films with the same mass (0.5±0.05 g), thickness (100±5 μm) and surface area (57 cm^2) were tested under the following experimental conditions: initial 4-aminophenol

concentration (50 ppm), temperature (273 – 313 K with 10 K increments). This allowed us to determine of the activation energy of sorption from the sorption rate constants at different temperatures. Kinetics sorption data was collected and analyzed with a kinetic model in addition to the intra-particle diffusion model.

3.7 Effect of NaCl

Sorbent films with the same masses (0.77±0.05 g), thicknesses (145±5 μm) and surface areas (57 cm^2) were prepared to see NaCl effect on sorption kinetics and equilibrium. This was performed at two different initial 4-aminophenol concentrations (50 and 500 ppm) and different NaCl concentrations from 0 – 2 wt%.

A preliminary study was performed to ensure that no overlap of UV-Vis absorption spectrums occurs for 4-aminophenol and NaCl at 296 nm. A UV-Vis spectrum at 200 – 700 nm wavelengths was generated with an aqueous solution containing only 1000 ppm of 4-aminophenol and then repeated with a solution containing only 2 wt% of NaCl. It was noted that neither spectrum curves infringed on each other at 296 nm. Furthermore, an aqueous solution containing both 1000 ppm of 4-aminophenol and 2 wt% of NaCl had the same spectrum plot as the aqueous solution which only contained 1000 ppm of 4-aminophenol. This suggests that it was appropriate to use the UV/Vis-Spectrophotometer to measure the concentration of 4-aminophenol in this study. Eq. **(11)** was used to calculate 4-aminophenol concentrations over time.

3.8 PEBA Sorbent Regeneration

The sorbent films with the same masses (1.184 ±0.02 g), thicknesses (240 ±5 μm) and surface areas (57 cm^2) were prepared to study regeneration of spent PEBA sorbent for repeated uses after exposure to 850 ppm of 4-aminophenol solutions. 100 mL of pure water and isopropanol (99% w/v) were used as regenerating agents. Sorption took place over 2 hours, then desorption took place over 2 hours, then the sorbent was dried for 1 hour and weighed. This was considered 1 "run". In total 3 sorption/desorption "runs" were performed on the sorbent consecutively.

Chapter 4

Results and Discussion

4.1 Sorption Isotherm Modelling

The sorption isotherm for 4-aminophenol and PEBA sorbent is shown in **Fig. 6** at temperatures 293 – 313 K and a concentration range of 300 – 3000 ppm. For each data point, equilibrium was considered once sorption did not change after waiting for 30 minutes.

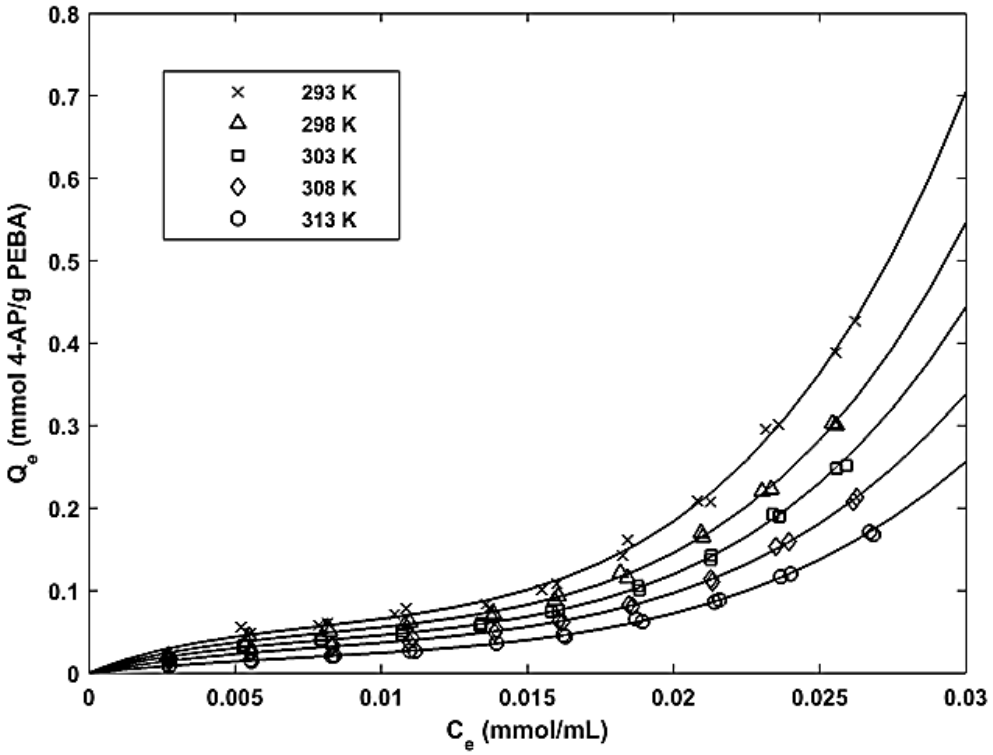

Fig. 6 Sorption isotherms of 4-aminophenol in PEBA at 293 – 313 K. Symbols: experimental data, solid lines represent model fitting based on a combined Langmuir and Freundlich model.

As temperature increased, the sorption capacity of 4-aminophenol on PEBA decreased at all feed concentrations, which signified that the sorption process is exothermic. In addition, a plateau is

observed up to an equilibrium concentration of 0.015 mmol/mL. Above that point the sorption isotherm spikes significantly, suggesting a change in the sorption mechanism.

The isotherm data was fitted with both the Langmuir and Freundlich isotherm models separately, as shown in **Fig. 7** and **Fig. 8** using Eq. (7) and (10) respectively. The clear poor linearity of the model fit calls for the search for an alternative model.

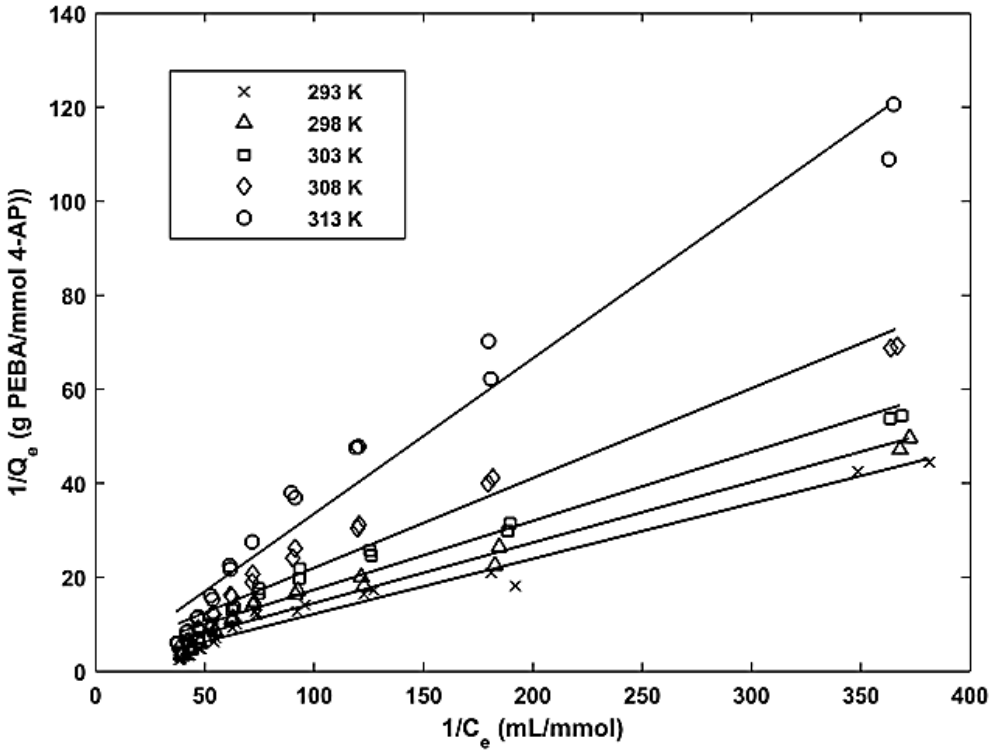

Fig. 7 Langmuir model fitting of 4-aminophenol sorption on PEBA.

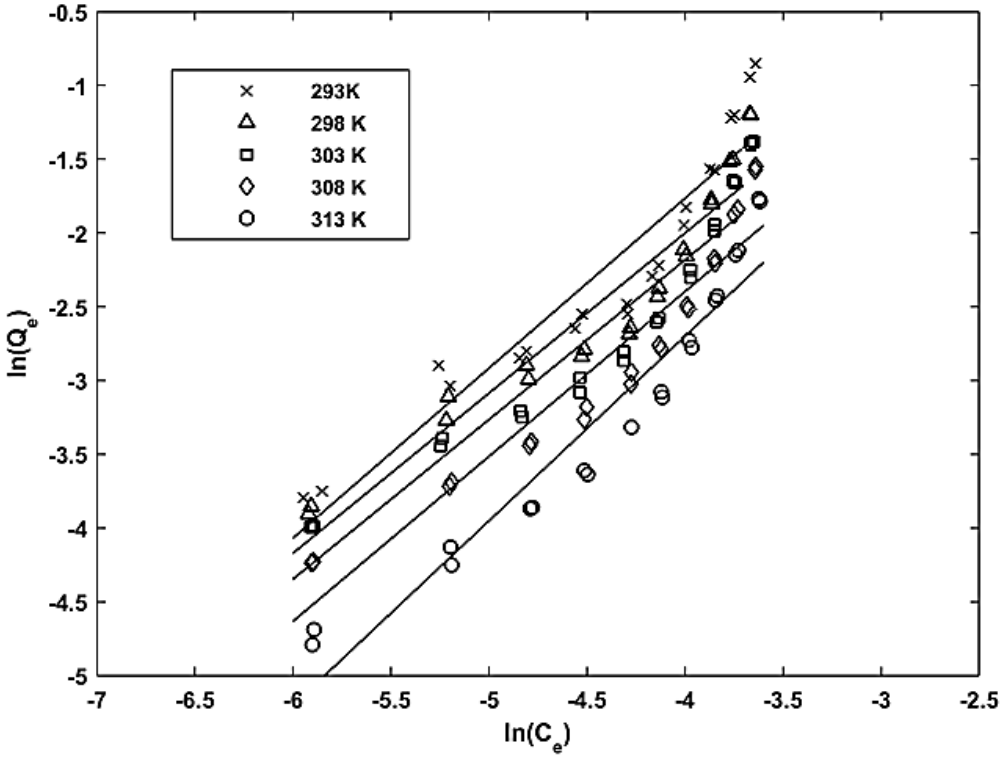

Fig. 8 Freundlich model fitting of 4-aminophenol sorption on PEBA.

An observed shape of the sorption isotherm curves was noticed where the first half resembled a Langmuir model (i.e., linearity in the first half of **Fig. 7**) and the second half resembled a Freundlich model (i.e., linearity in the second half of **Fig. 8**). A data fit combining both models was performed using Eq. (18) and is seen alongside the experimental data in **Fig. 6.**

$$Q_e = \left(\frac{Q_m \cdot K_L \cdot C_e}{1 + K_L \cdot C_e}\right) + \left(K_f \cdot C_e{}^{\frac{1}{n}}\right) \qquad \textbf{(18)}$$

The combined model parameters were determined using a non-liner regression technique derived in MATLAB, and the results are displayed in **Table 3**.

Table 3 Langmuir and Freundlich combined model fitting parameters and statistical analysis for 4-aminophenol on PEBA sorbent.

Temperature (K)	Langmuir		Freundlich		R^2
	Q_m (mmol·g^{-1})	K_l (mL·mmol^{-1})	K_F x 10^5 (dimensions based on n)	$^1/_n$	
293	0.0970	163.6	21.5	4.29	0.9973
298	0.0873	144.9	21.5	4.37	0.9983
303	0.0741	135.5	16.7	4.36	0.9992
308	0.0675	101.6	8.07	4.23	0.9991
313	0.0524	72.71	4.32	4.13	0.9994

The combined model fit is suitable for this system with high R^2 values (> 0.995) at all temperatures. The quantity Q_m decreased with an increase in temperature, representative of the first plateau shown in the isotherm. In addition, K_F decreased with an increase in temperature, indicating an exothermic sorption process, whereas $^1/_n$ remains similar at different temperatures.

The sorption isotherm curves seem to indicate multiple sorption scenarios occurring during sorption. According to an isotherm classification proposed by Giles et al, an S3 curve is formed with monohydric phenols sorbed onto polar substrates from a polar solvent. In this case the sorption becomes easier as the concentration increases [54]. 4-aminophenol is a monohydric phenol and water is a polar molecule, but PEBA is not a steadily polar substrate. It contains highly polar polyamide segments, but the remaining polyether segments are less polar. This discrepancy in consistency of surface polarity could explain why the isotherm for 4-aminophenol sorption on PEBA is not an exact representation of an S3 curve, but does share a similar shape. The initial stage from a C_e of 0 mmol/mL to 0.0025 mmol/mL represents the beginning of the S3 curve, where "co-operative adsorption" may be occurring. This means that side-by-side association between sorbed molecules becomes more apparent as the solution concentration

increases, which increases the affinity for the bulk 4-aminophenol as more is sorbed to the surface of the PEBA [54]. After a C_e of 0.0025 mmol/mL, a relatively long plateau begins to form, which according to Giles et al. means that the initial monolayer formed has a low attraction for additional solute to sorb to this new surface. Finally, the last section of the isotherm (after C_e = 0.015 mmol/mL) which rises steadily with no discernible plateau could signify multilayer formation, where the new surfaces formed show high attraction for bulk phenol solute.

Since the first half of the combined isotherm model primarily uses the traditional Langmuir model parameters, the monolayer formation on the surface of the sorbent (from C_e = 0.0025 to 0.015 mmol/mL) can be explained according to Langmuir sorption theory (see **Section 3.2**). The second half of the combined isotherm mainly uses the traditional Freundlich model parameters, which can explain multilayer formation occurring on the sorbent (after C_e = 0.015 mmol/mL) according to Freundlich sorption theory (see **Section 3.3**).

4.2 Sorption Kinetics at Different Initial Concentration

To find a suitable model for sorption kinetics of 4-aminophenol on PEBA, two kinetic models were primarily considered: pseudo-first order and pseudo-second order sorption kinetics. The sorption kinetics data are shown in **Fig. 9** where 4-aminophenol uptake over time at different initial 4-aminophenol concentrations.

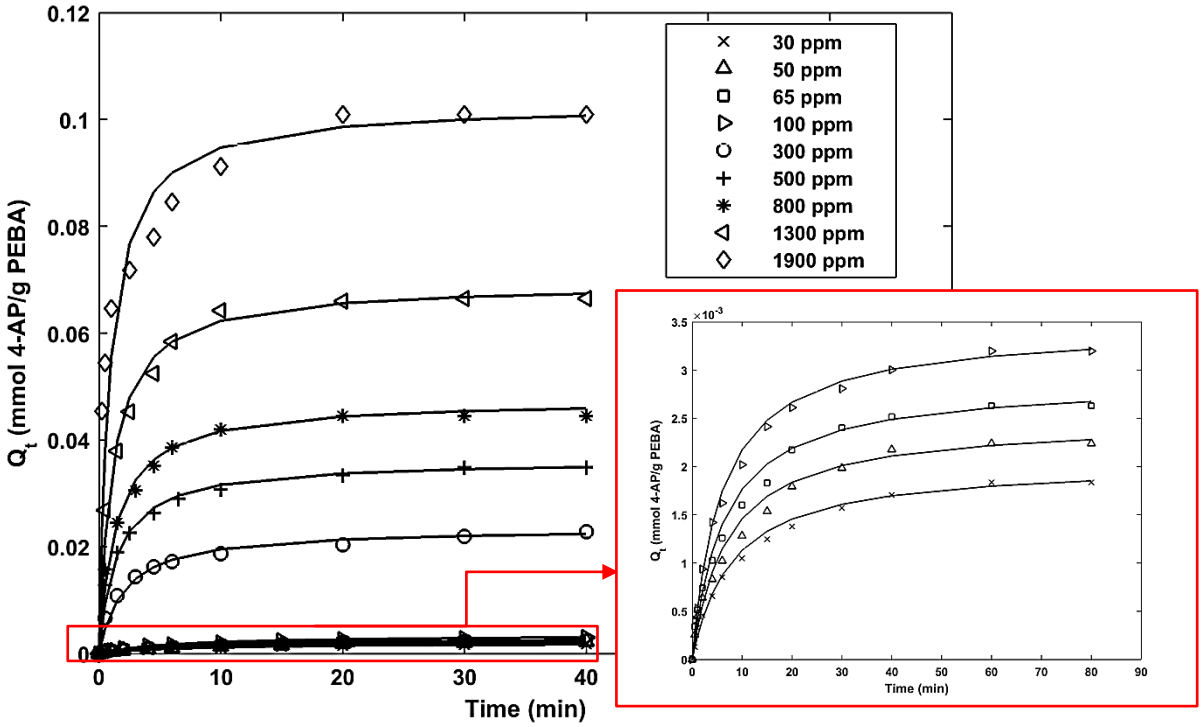

Fig. 9 Experimental data for the sorption of 4-aminophenol at different initial concentrations at 293 K. Solid lines represent pseudo-second order model fit.

The experimental data was fitted to Eq. (13) for the pseudo-first order (**Fig. 10**) and Eq. (15) for the pseudo-second order (**Fig. 11**) models, respectively.

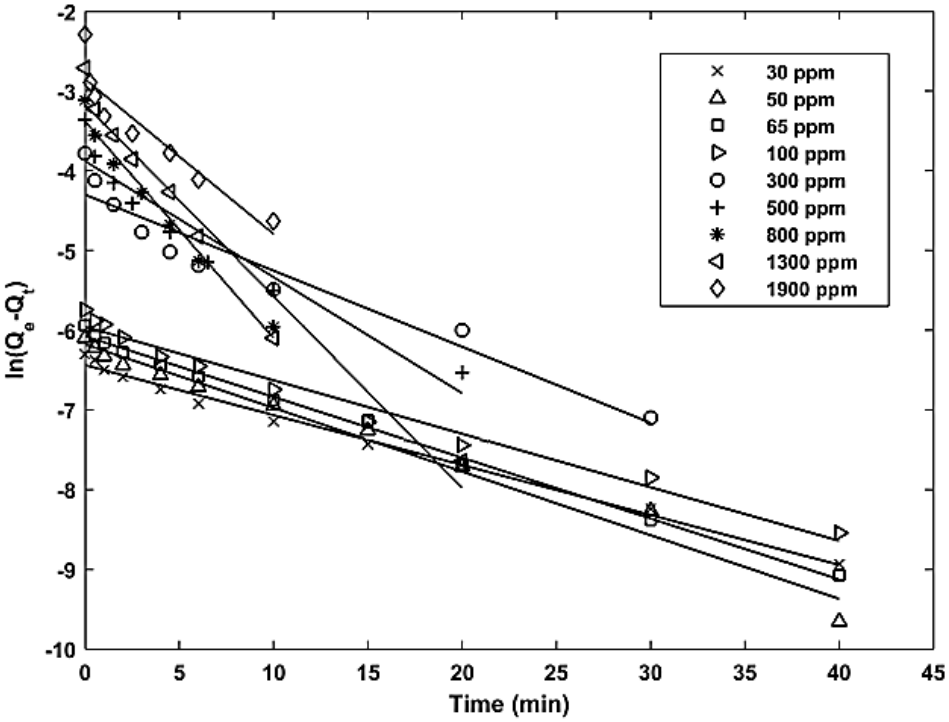

Fig. 10 Linearized pseudo-first order model for 4-aminophenol sorption on PEBA at different initial concentrations.

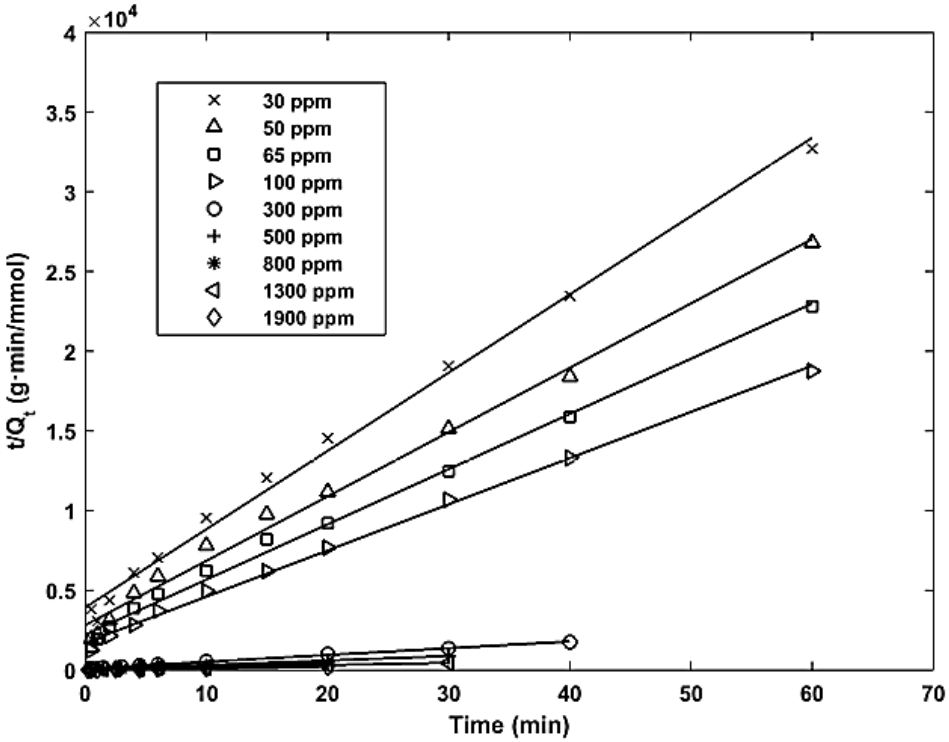

Fig. 11 Linearized pseudo-second order model for 4-aminophenol sorption on PEBA at different initial concentrations.

Table 4 Parameters for kinetic sorption models.

Initial Conc. (ppm)	Pseudo-First Order			Pseudo-Second Order			Experimental Q_e (mmol·g^{-1})
	K_1 (min^{-1})	Q_e (mmol·g^{-1})	R^2	K_2 (g·mmol^{-1}·min^{-1})	Q_e (mmol·g^{-1})	R^2	
30	0.0625	0.00159	0.9924	65.54	0.00202	0.9929	0.00184
50	0.0792	0.00203	0.9793	62.88	0.00245	0.9911	0.00224
65	0.0762	0.00229	0.9954	54.42	0.00289	0.9940	0.00263
100	0.0669	0.00257	0.9786	50.98	0.00344	0.9969	0.00320
300	0.0954	0.0135	0.9222	22.81	0.0235	0.9982	0.0228
500	0.145	0.0206	0.9208	18.97	0.0362	0.9992	0.0348
800	0.272	0.0339	0.9766	15.23	0.0475	0.9991	0.0445
1300	0.314	0.0521	0.9649	12.96	0.0693	0.9994	0.0665
1900	0.196	0.0574	0.8727	11.73	0.103	0.9958	0.101

The kinetic model parameters and R^2 values for the model fitting, in addition to equilibrium uptake (Q_e) measured and the values predicted by the models, are presented in **Table 4**. The pseudo-second order model appears to be appropriate for the sorption of 4-aminophenol on PEBA sorbent with high R^2 values (>0.991) for all the fits, and the quantity Q_e values determined from the data fitting are closer to those obtained from experiments. It is possible to use this model to predict the sorption of 4-aminophenol on PEBA sorbent, and a comparison of model calculations and corresponding experimental data is shown in **Fig. 9**.

Even though the pseudo-second order model seems to fit the data well, it is important to note that the second order rate constant (K_2) is shown to change as the initial solute concentration changes. However, in integrating the differential pseudo second order model equation to yield

Eq. **(15)**, it was implied that the K_2 is a constant in regards to concentration. Two separate approaches were attempted in order to combat this discrepancy[1]:

1) The K_2 "constant" was redefined as a "pseudo-constant" by solving it as an implicit function of initial concentration
2) The equilibrium uptake (Q_e) term in the pseudo-second order model, which was also treated as a constant in the linearized integrated model equation, was re-considered as a variable value which changes as sorption proceeds, corresponding to instantaneous solute concentration

Following the first approach mentioned, a plot of the K_2 values against the initial solute concentration were fitted to a power function using a non-linear regression function written in MATLAB (**Fig. 12**):

$$K_2 = 1.6458 \cdot (C_o)^{-0.469} \quad \textbf{(19)}$$

Other studies also show similar results where K_2 is a function of C_o [55 - 57], most notably for the sorption of Pb(II) onto peat where the second order rate constant against initial concentration followed a power line fit as well [58]. Azizian derived the pseudo-second order kinetic model with K_2 being a function of the initial solute concentration, and the adsorption and desorption

[1] The pseudo-second order model, as opposed to choosing a different kinetic model, continued to be the primary model because of its initial appropriate fit to the experimental data (**Fig. 9**) and its semi-empirical nature gives meaning to the values obtained allowing for further analysis (ie. activation energy).

rate constants were determined [59]. This function in its entirety was simplified and represented as follows:

$$K_2 = (2Q_e)^{-1}\left[k_a\left(\beta + C_o + \frac{1}{K}\right) - \sqrt{\left(-k_a\left(\beta + C_o + \frac{1}{K}\right)\right)^2 - (4k_a^2 \cdot \beta \cdot C_o)}\right] \quad \textbf{(20)}$$

where

$$\beta = \frac{(C_o - C_e)(1 + K \cdot C_e)}{K \cdot C_e} \quad \textbf{(21)}$$

K (mL/mmol) is the true equilibrium constant and k_a (mL/mmol·min) is the sorption rate constant. It is then possible to use:

$$K = \frac{k_a}{k_d} \quad \textbf{(22)}$$

to determine the desorption rate constant k_d (min^{-1}). Eq. **(20)** and Eq. **(21)** were applied to the 4-aminophenol/PEBA sorption kinetic data, and the following results were obtained: equilibrium constant 741.6 mL/mmol, and sorption and desorption rate constants 79.5 mL/mmol·min and 0.107 min^{-1}, respectively. It is important to note that this newly calculated equilibrium constant is now independent of initial concentration of 4-aminophenol. In addition, there is good reproducibility of the K_2 values when predicting them with the Azizian model, including an R^2 of 0.9798 when comparing them to the experimental K_2 values (see **Fig. 12**).

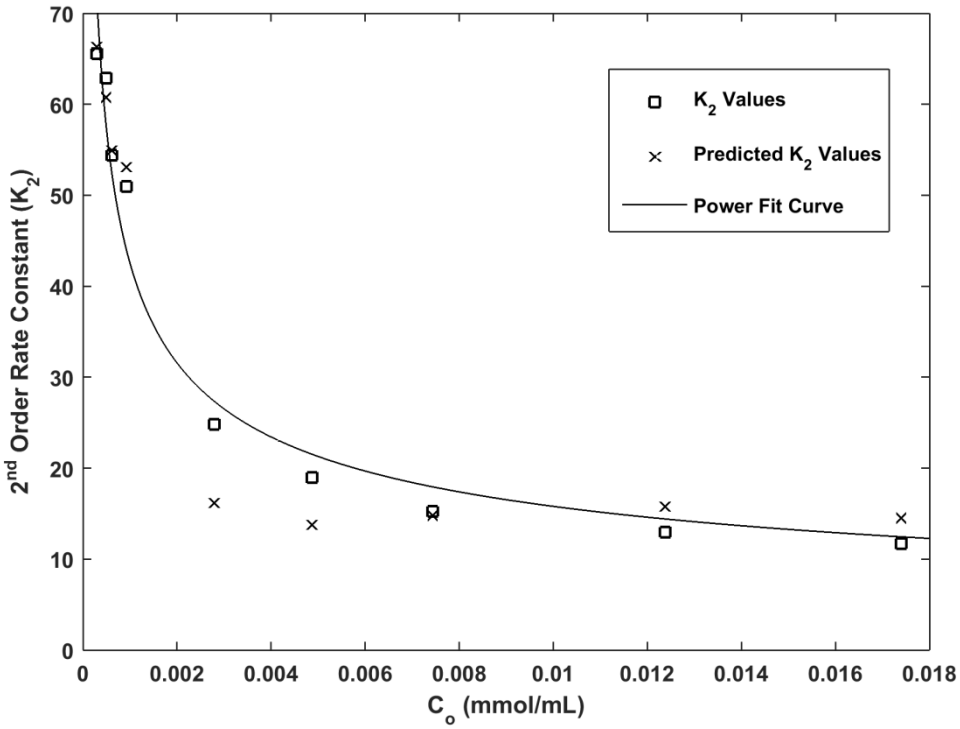

Fig. 12 Second order rate constant K_2 and its corresponding power fit line versus initial 4-aminophenol concentration alongside K_2 values predicted by the Azizian derived model.

The second approach mentioned earlier will now be attempted. It is clear that the 4-aminophenol concentration in the bulk solution decreased as sorption proceeded in a batch process. This means that equilibrium uptake (Q_e) changes during this time as well and should not be considered a constant in the pseudo-second order model. Instead it will be modified using a function of instantaneous solute concentration. In **Section 4.1** it was determined that the 4-aminophenol/PEBA system fits well to the combined Langmuir-Freundlich isotherm model (Eq. **(18)**) which represents the relationship between Q_e and C_e. Furthermore, the mass balance equation of a batch sorption process can be described by Eq. **(11)**, which can be rearranged into the following equation:

$$C_t = C_o - \frac{Q_t M}{V} \quad \textbf{(23)}$$

The corresponding Q_e can now be represented as a function of Q_t by substituting Eq. **(23)** into Eq. **(18)**[2].

$$Q_e = \left(\frac{Q_m \cdot K_L \cdot \left(C_o - \frac{Q_t M}{V}\right)}{1 + K_L \cdot \left(C_o - \frac{Q_t M}{V}\right)}\right) + \left(K_f \cdot \left(C_o - \frac{Q_t M}{V}\right)^{\frac{1}{n}}\right) \quad \textbf{(24)}$$

Substituting Eq. **(24)** into the pseudo-second order model (Eq. **(14)**).

$$\frac{dQ_t}{dt} = K_2'\left(\left[\left(\frac{Q_m \cdot K_L \cdot \left(C_o - \frac{Q_t M}{V}\right)}{1 + K_L \cdot \left(C_o - \frac{Q_t M}{V}\right)}\right) + \left(K_f \cdot \left(C_o - \frac{Q_t M}{V}\right)^{\frac{1}{n}}\right)\right] - Q_t\right)^2 \quad \textbf{(25)}$$

The rate constant K_2' was then recalculated using the Q_m, K_L, K_f and $^1/n$ parameters taken from the isotherm parameters shown in **Table 3** at 298K. The kinetic data were fitted to the differential equation using Matlab, and the resulting model parameters are shown in **Table 5.** The predicted sorption uptake is compared with experimental data, as shown in **Fig. 13**.

[2] C_e will be exchanged by C_t during this substitution in Eq. **(18)** so it corresponds to instantaneous solute concentration.

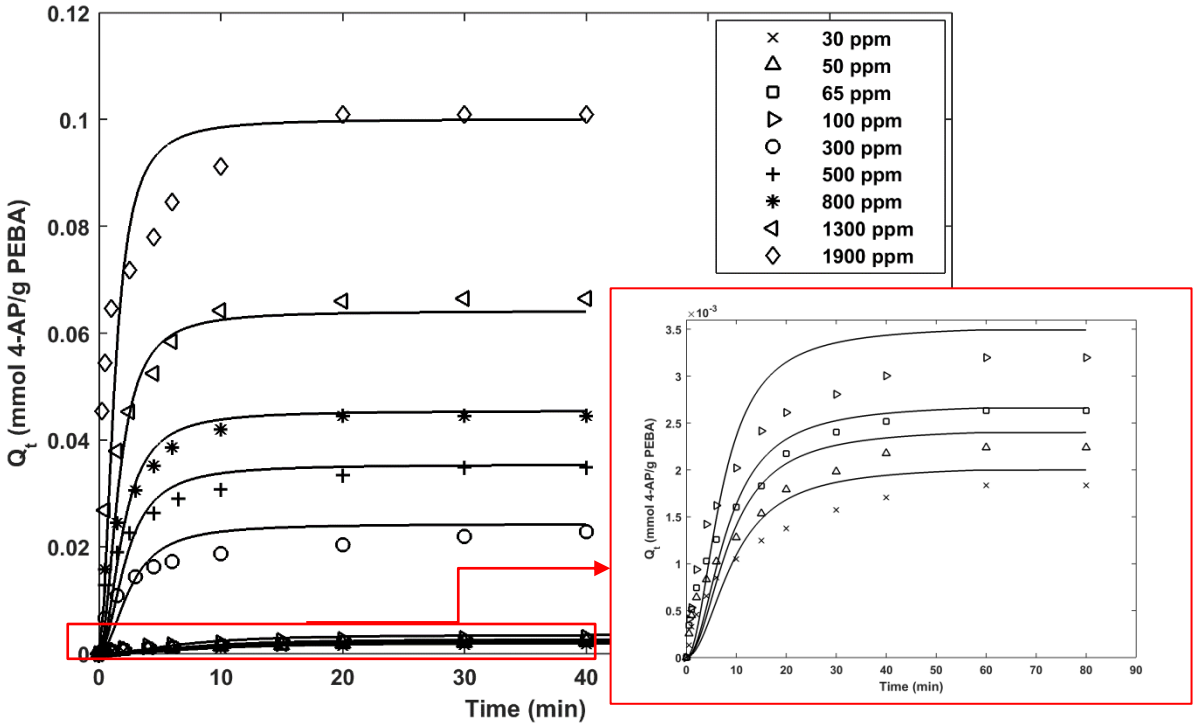

Fig. 13 Modified pseudo-second order model predicted uptake against experimental uptake at different 4-aminophenol concentrations.

Table 5 Rate constant determined from modified pseudo-second order kinetic sorption model.

Initial Conc. (ppm)	Modified Pseudo-Second Order		Experimental Q_e (mmol·g^{-1})
	K_2' (g·mmol^{-1}·min^{-1})	R^2	
30	10.762	0.8662	0.001836
50	10.582	0.8634	0.002240
65	10.710	0.8589	0.002632
100	10.644	0.8775	0.003198
300	10.736	0.7947	0.02279
500	10.739	0.8083	0.03484
800	10.972	0.8699	0.04450
1300	10.815	0.8622	0.06649
1900	10.896	0.3705	0.1009

The newly recalculated K_2' parameter can be considered a constant independent of solute concentration with a value of about 10.7 g/mmol·min. However, the data fitting shown in **Fig. 13** showed lower R^2 values (see **Table 5**) when compared with the data fitting with unmodified model.

The remaining sections within this study did not use the alternate methods to calculate the K_2 rate constants, and instead opted for the unmodified pseudo-second order model. This is because neither alternate method offered a flawless solution to find K_2 while the unmodified model gave a fairly good data fit. The K_2 values were only compared relative to one another since the values themselves did not offer any intrinsic meaning.

The kinetic data was analyzed with the intra-particle diffusion model (Eq. **(16)**) as well by only considering the initial stages of the sorption process (< 50% uptake for below 100 ppm and < 70% uptake for above 100 ppm). This is shown in **Fig. 14,** and the model parameter determined from the data fitting based on the intra-particle diffusion model are shown in **Table 6**.

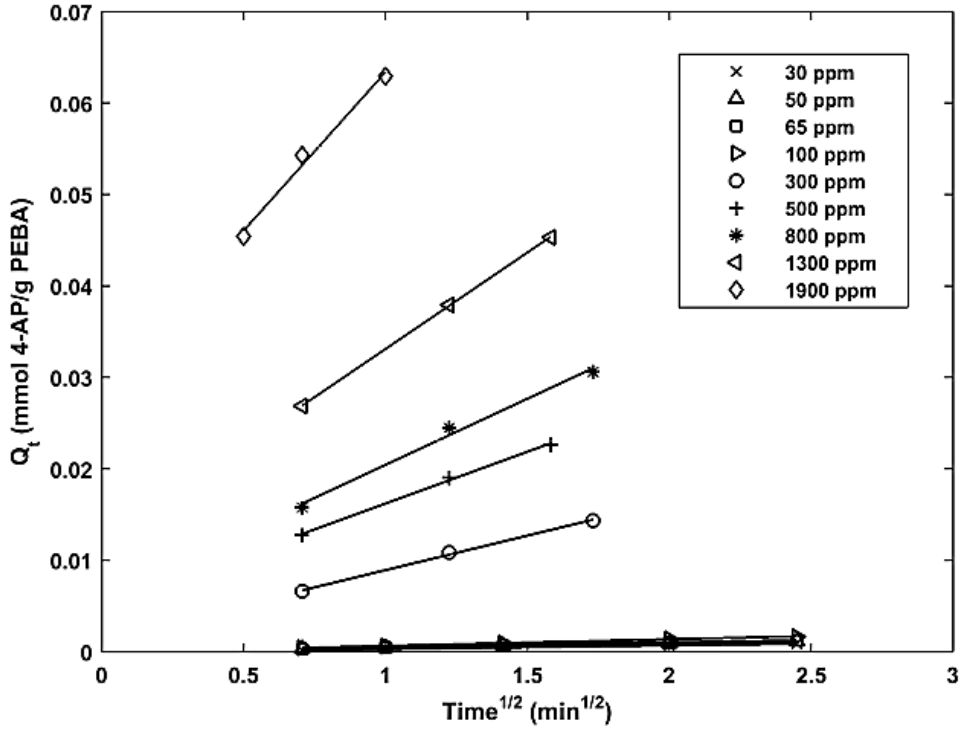

Fig. 14 Data fit to the intra-particle diffusion model for sorption of 4-aminophenol on PEBA at different initial 4-aminophenol concentrations.

Good linearization of the data in Fig. 14 indicates that 4-aminophenol sorption in PEBA involves diffusion into the sorbent interior. If diffusion was the only rate-limiting mechanism, then the straight line would pass through the origin, this is shown to not be the case [60]. This is more easily emphasized by looking at the values of parameter *C* which increases by two orders of magnitude above 100 ppm. It must be noted that this doesn't undermine potential diffusion effects at concentrations below 100 ppm, but the effect is far more pronounced above this concentration. Diffusion is working alongside other mechanism for rate of sorption.

The intra-particle diffusivity, D_c, was determined using Eq. (17) based on the sorption kinetics data re-plotted in **Fig. 15**, and the values are shown in **Table 6**. The diffusivity is shown to increase with an increase in the solute concentration. This is understandable if diffusion is the rate controlling step because an increase in the solute concentration will increase the sorption

uptake in the sorbent, thereby causing swelling of the sorbent which makes it easier for diffusion of solute molecules.

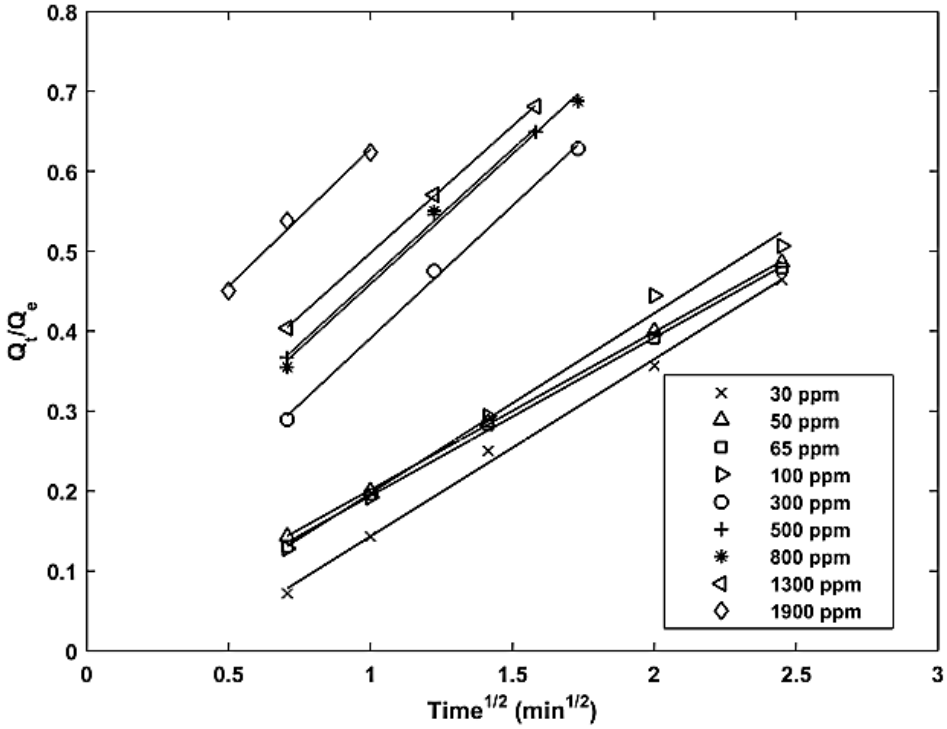

Fig. 15 Fractional sorption uptake versus $t^{1/2}$ for 4-aminophenol sorption on PEBA at different initial 4-aminophenol concentrations.

Table 6 Parameters for diffusion models of different initial concentrations of 4-aminophenol on PEBA sorbent.

Initial Conc. (ppm)	Model parameters based on intra-particle diffusion		Intra-particle Diffusivity	R^2
	k_i ($mmol \cdot g^{-1} \cdot min^{-1/2}$)	C ($mmol \cdot g^{-1}$)	D_c x 10^{10} ($m^2 \cdot min^{-1}$)	
30	3.712E-04	-6.908E-05	0.828	0.9983
50	4.421E-04	8.979E-06	0.932	0.9998
65	5.212E-04	-1.110E-05	1.085	0.9989
100	7.204E-04	-9.032E-05	1.601	0.9923
300	7.547E-03	1.367E-03	3.066	0.9975
500	1.133E-02	4.868E-03	3.214	0.9976
800	1.446E-02	5.965E-03	3.342	0.9911
1300	2.109E-02	1.200E-02	3.579	0.9999
1900	3.467E-02	2.871E-02	3.734	0.9889

4.3 Surface Adsorption or Bulk Sorption

Fig. 16 shows the sorption uptake in sorbent films of the same masses but with different surface areas. It was shown that the same sorption capacity was obtained when the sorption reached equilibrium.

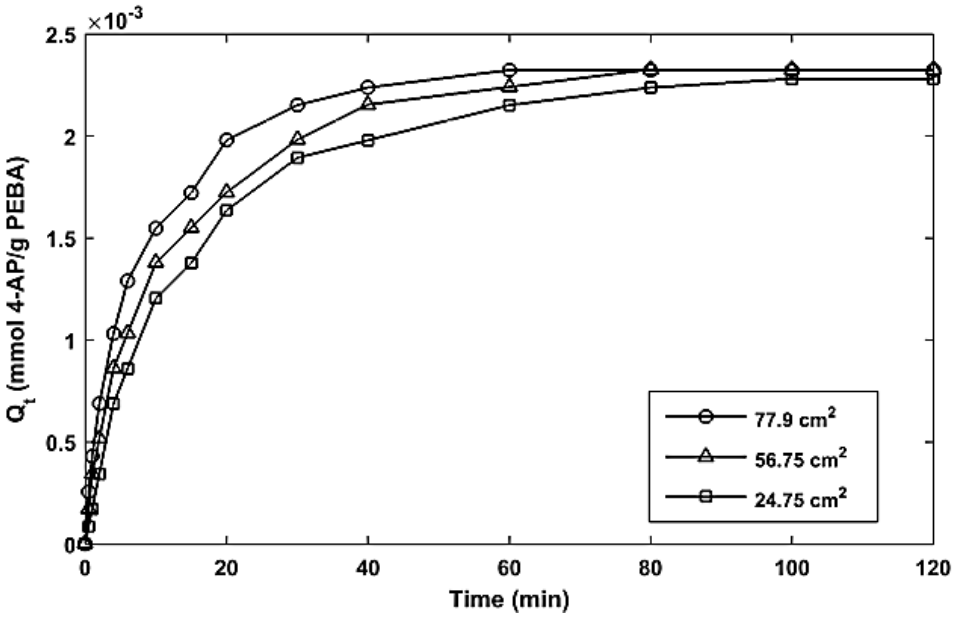

Fig. 16 Uptake of 4-aminophenol on 0.778 g PEBA sorbent films with different surface areas.

This means that the sorption uptake is not a surface phenomenon (i.e., adsorption), but rather internal sorption in the sorbent bulk had occurred. The Pseudo-second order kinetic analysis was performed based on the original unmodified linearized plot displayed in **Fig. 17,** and the corresponding model parameters are shown in **Table 7**.

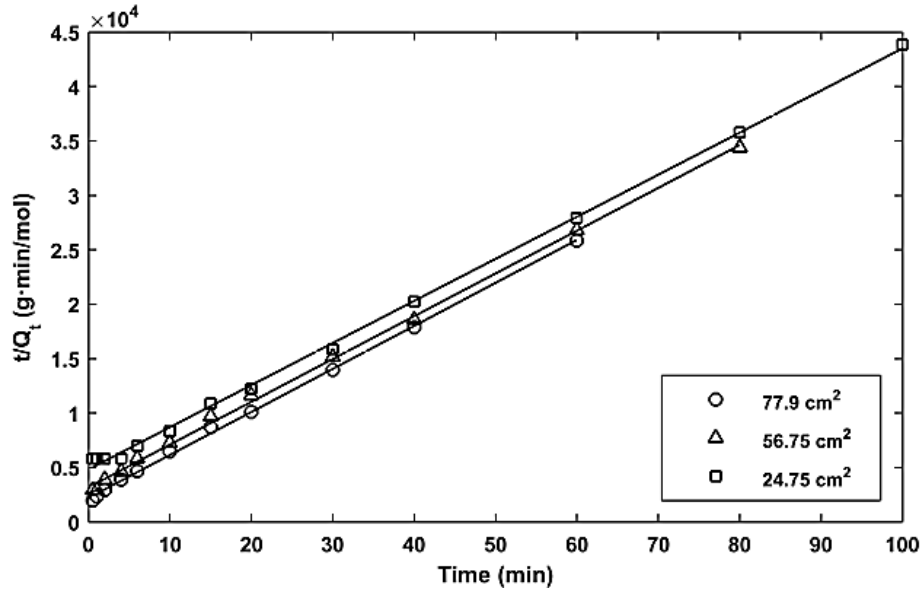

Fig. 17 Linearized pseudo-second order model for data from **Fig. 16**.

In spite of the shortcomings of the unmodified model, the Q_e predicted by the model is close to the experimental value. The pseudo-second order rate constant, K_2, is shown to increase as surface area increased. This is expected because as mentioned earlier, for sorbent films with a given mass, a larger surface area means a thinner film, and thus sorption uptake rate increases. This also indicates that the sorption is not merely a surface "reaction" mechanism, and internal mass transfer in the bulk of the sorbent is not negligible. On the other hand, when evaluated with the intra-particle diffusion model, the diffusivity coefficient (as shown in **Table 7)** is shown to be influenced by the film thickness. This suggests that intra-particle diffusion is not the only mechanism of sorption either. This supports the points made in **Section 4.2**. As the sorbent film thickness increases, the intra-particle diffusivity decreases. This could be because the rate of sorption occurring on the surface of the sorbent is higher than the rate of intra-particle diffusion. Therefore, the calculated diffusion coefficient, which is an apparent quantity, is inflated due to the more significant effect of surface reaction on the PEBA sorbent.

Table 7 Sorption kinetic parameters based on pseudo-second order and intra-particle diffusion models for sorbent films with different surface areas and the same masses (0.777 g).

Surface Area (cm^2)	Pseudo-Second Order			Intra-particle Diffusion				Experimental Q_e ($mmol \cdot g^{-1}$)
	K_2 ($g \cdot mmol^{-1} \cdot min^{-1}$)	Q_e ($mmol \cdot g^{-1}$)	R^2	k_i ($mmol \cdot g^{-1} \cdot min^{-1/2}$)	C ($mmol \cdot g^{-1}$)	D_c x 10^{10} ($m^2 \cdot min^{-1}$)	R^2	
77.9	30.98	0.002586	0.9989	6.009E-4	-1.670E-4	9.4875	0.9998	0.002323
56.75	48.76	0.002544	0.9985	4.997E-4	-1.707E-4	2.1754	0.9958	0.002326
24.75	71.16	0.002531	0.9986	4.649E-4	-2.738E-4	1.2614	0.9911	0.002280

To further support that diffusion is not the only mass transport mechanism for the sorption within the PEBA sorbent, three identical sorbent films with the same mass (0.770 g) and thickness (127 μm) were tested for 4-aminophenol sorption in 100 ml of aminophenol solution at an initial concentration of 50 ppm. One of them was sliced into numerous evenly sized pieces measuring 2 mm x 30 mm, and another was sliced into smaller pieces of 2 mm x 2 mm. The sorption kinetics was monitored over time, and the sorption uptake during the course of sorption is shown in **Fig. 18**.

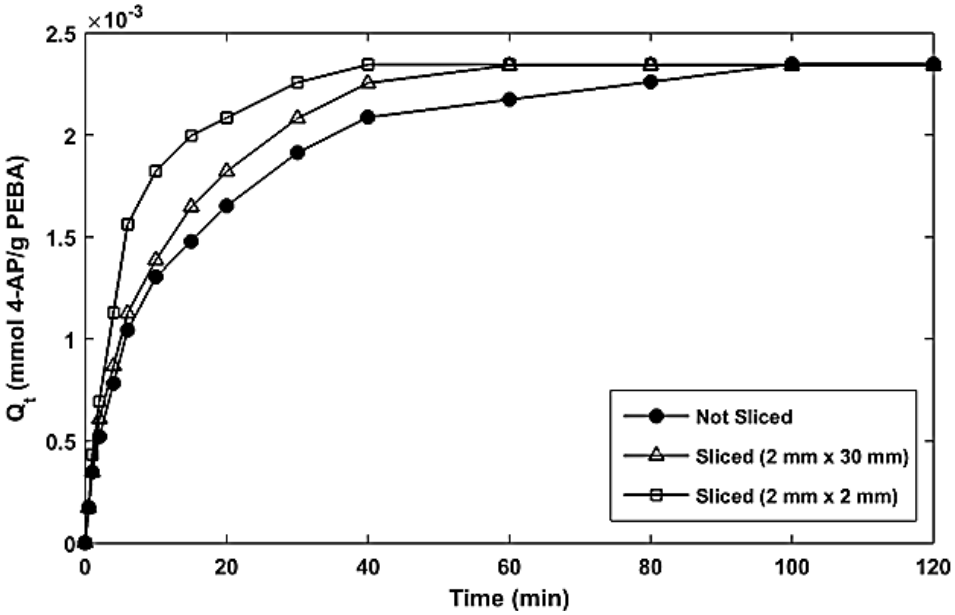

Fig. 18 Sorption of 4-aminophenol in PEBA with and without slicing the PEBA sorbent films (mass 0.771 g and thickness 127 μm) into evenly sized pieces.

As expected, the same uptake capacity (0.00234 mmol/g) at equilibrium was reached. The only discerning difference between the sliced sorbent films and the unsliced sorbent film is the additional external surface areas created by slicing the sorbent films into small pieces. When the equilibrium sorption uptake on PEBA sorbent with the same sorbent masses but different surface areas and thicknesses is normalized by their external surface area, as shown in **Fig. 16** ,it is apparent that the sorption uptake is not determined by the surface area, indicating again that the

sorption is not via a surface adsorption mechanism, consistent with the equilibrium sorption capacity data shown in Fig. 18.

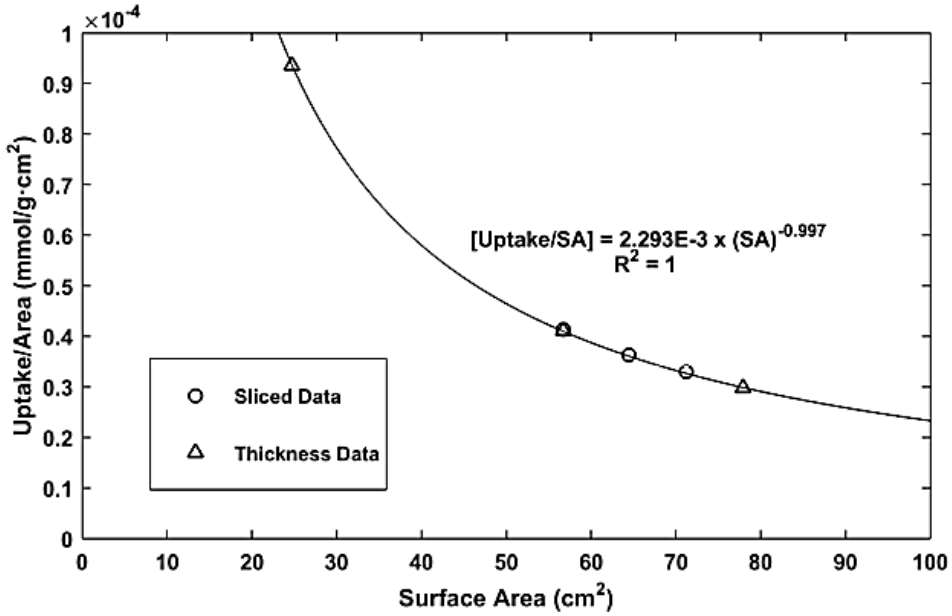

Fig. 19 Uptake per sorbent surface area versus sorbent surface area for sorption data found on **Fig. 18**.

Additional support towards internal sorption can be seen in **Fig. 20**.

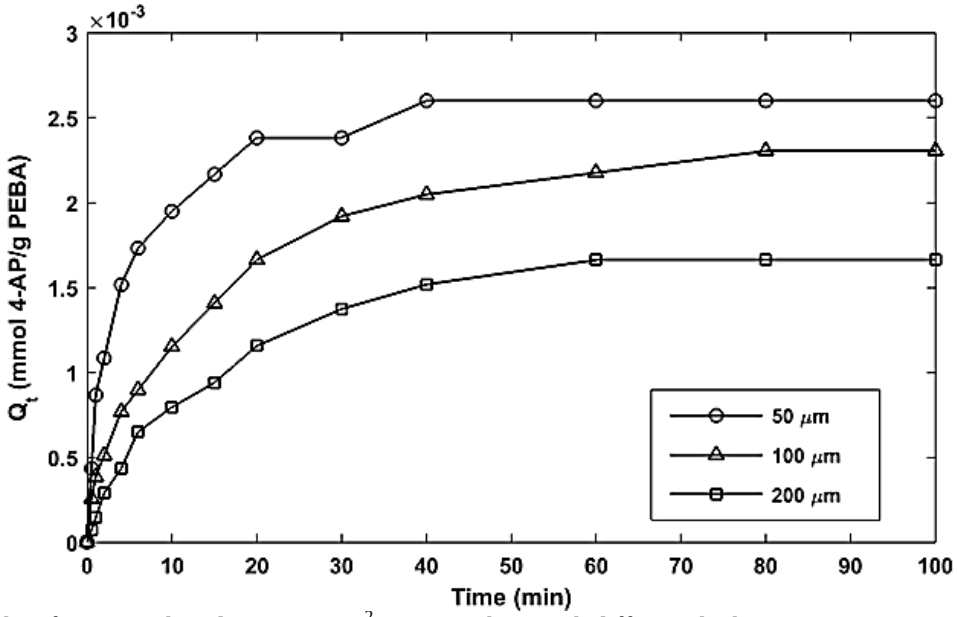

Fig. 20 Uptake of 4-aminophenol on 56.75 cm^2 PEBA sorbent with different thicknesses.

Changing the thickness of sorbent films while keeping surface area constant showed differing uptakes of 4-aminophenol at sorption equilibrium, signifying internal sorption occurred in tandem with surface sorption. Uptake tended to decrease as thickness increased due to a lower equilibrium concentration being reached, thus lower sorption capacity at equilibrium. It also showed that thicker films had a slower sorption rate due to increased internal resistance to mass transfer pertaining to sorption.

4.4 Activation Energy

Sorption kinetics at different temperatures was determined to investigate the effect of temperature on the sorption rate, and the experimental data was shown in **Fig. 21**.

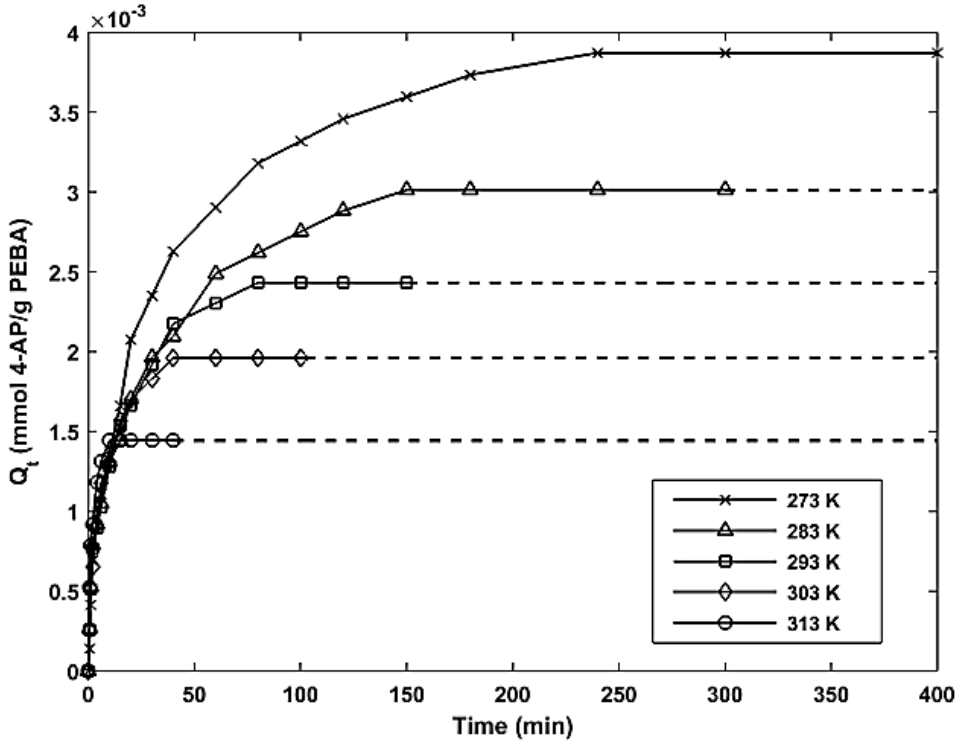

Fig. 21 4-aminophenol uptake at 50 ppm on PEBA with sorption times at various temperatures

A trade-off between sorption speed and sorption capacity was apparent as temperature changed. At 273 K the uptake capacity was the highest with 3.872×10^{-3} mmol/g while at 313 K it was the lowest with 1.444×10^{-3} mmol/g.

The activation energy of sorption can be calculated with the Arrhenius equation:

$$K = A \cdot e^{\left(\frac{-E_a}{R \cdot T}\right)} \quad \textbf{(26)}$$

where K is a rate constant, A is the temperature independent pre-exponential factor, R (kJ/mol·K) is the universal gas constant and T (K) is the temperature. Eq. **(28)** was rearranged into the following linear form:

$$\ln K = \ln A - \frac{E_a}{R \cdot T} \quad \textbf{(27)}$$

where ln(K) versus $^1/_T$ was plotted to determine E_a from the slope and A from the y-intercept.

If sorption was considered primarily diffusion controlled, then it was possible to predict activation energy, E_a (kJ/mol), for diffusion using an Arrhenius-type of equation [61]:

$$D_c = D_o \cdot e^{\left(\frac{-E_a}{R \cdot T}\right)} \quad \textbf{(28)}$$

where D_o is the temperature independent pre-exponential factor. Eq. **(28)** was rearranged into the following linear form:

$$\ln D_c = \ln D_o - \frac{E_a}{R \cdot T} \quad \textbf{(29)}$$

where $\ln(D_c)$ versus $^1/_T$ was plotted to determine E_a from the slope and D_o from the y-intercept.

Following analysis with pseudo-second order (**Fig. 22**) and diffusion (**Fig. 23**) models for sorption kinetics, the activation energy was determined using Eq. (27) and Eq. (29) from the best fit lines in **Fig. 24** and **Fig. 25**, respectively.

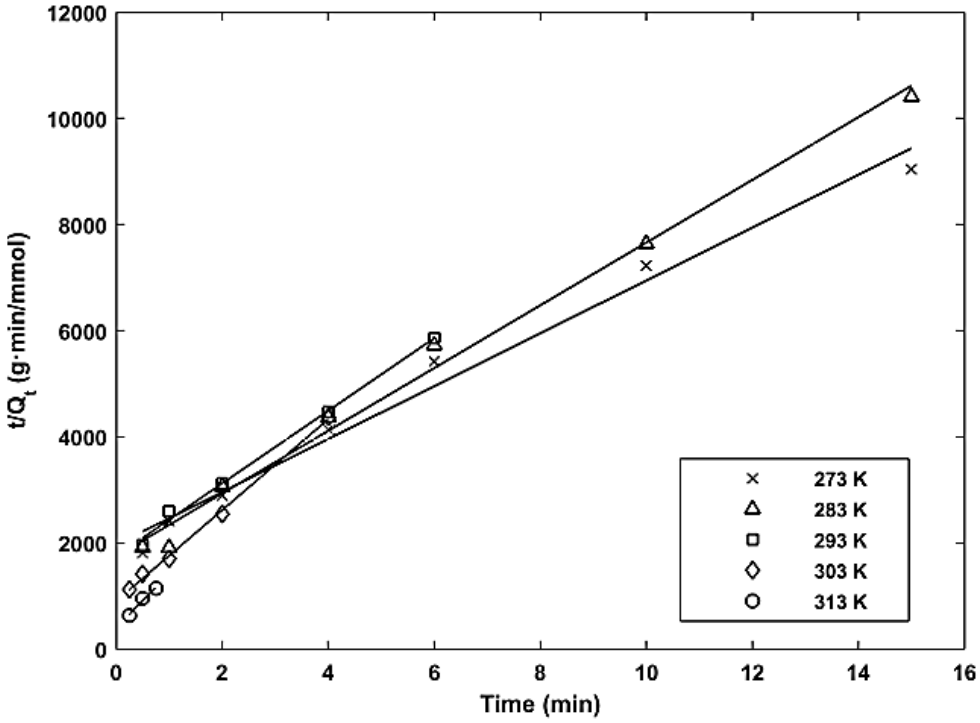

Fig. 22 t/Q_t versus time for 4-aminophenol sorption in PEBA at various temperatures.

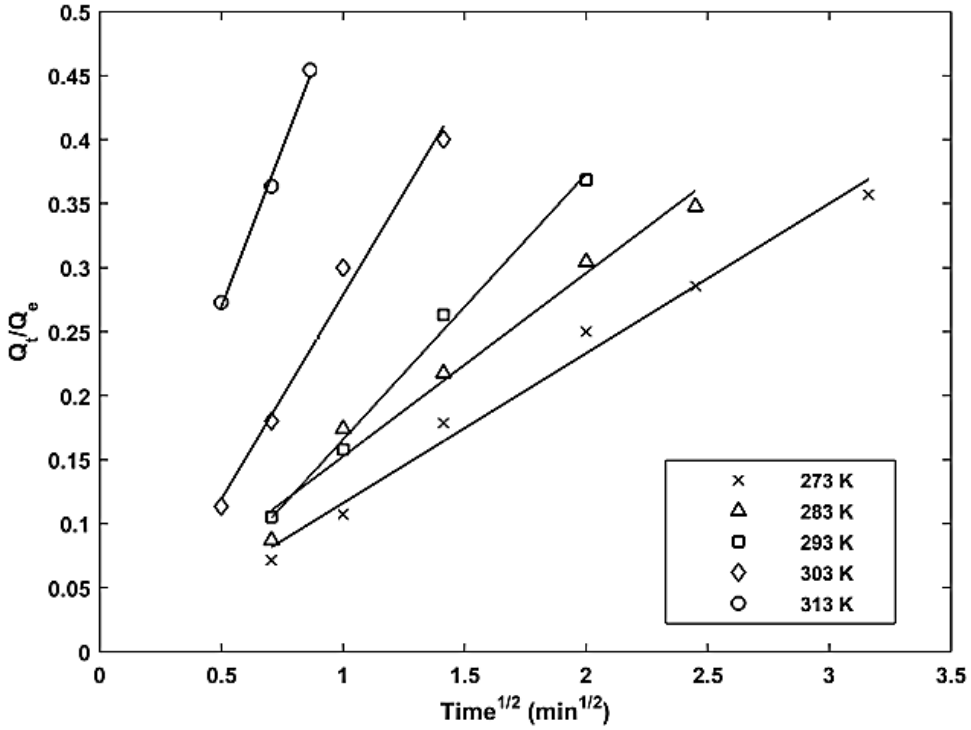

Fig. 23 Q_t/Q_e for 4-aminophenol sorption in PEBA at various temperatures.

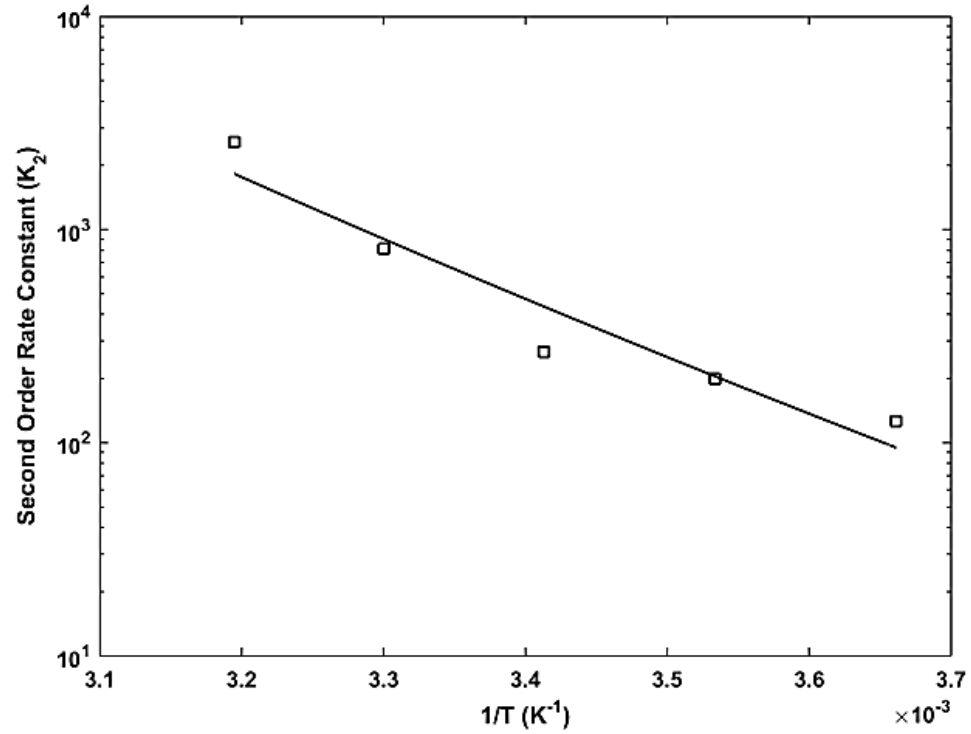

Fig. 24 K_2 versus 1/T for 4-aminophenol sorption in PEBA.

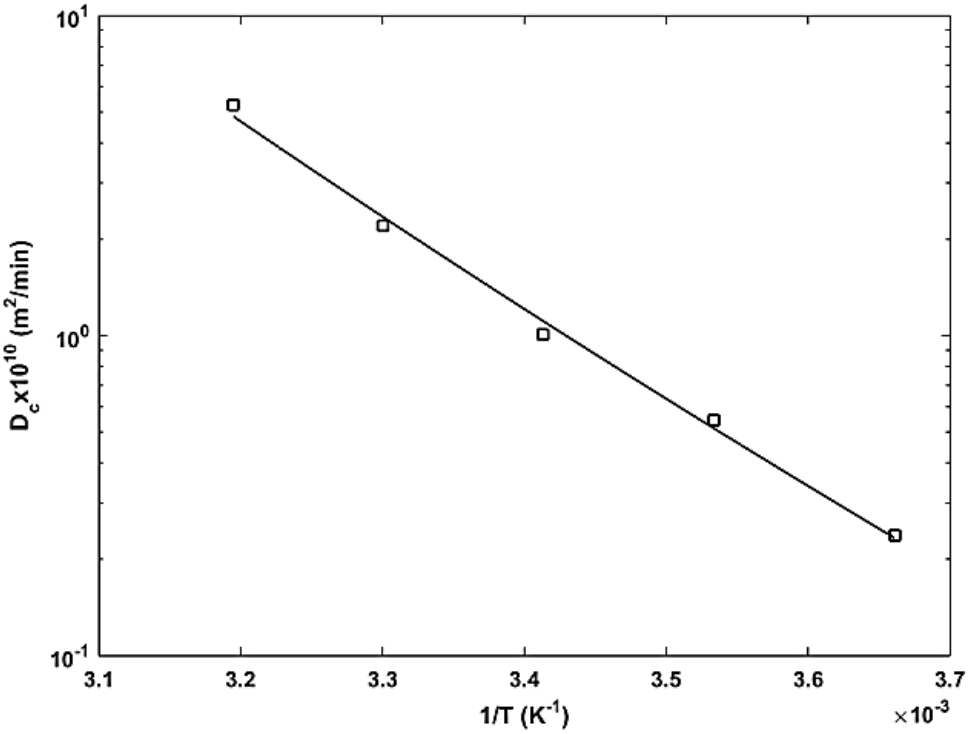

Fig. 25 D_c versus 1/T for 4-aminophenol sorption in PEBA.

Activation energy for sorption of 4-aminophenol on PEBA sorbent was similar no matter whether the second order rate constants were used (52.2 kJ/mol) or intra-particle diffusivities were used (54.0 kJ/mol). The slight discrepancy between these numbers is reasonable, because the pseudo second-order model is not entirely suitable for this system. The apparent second order rate constants could be underestimating the energy required for sorption. It would be more appropriate to use the true kinetic rate constant *K* calculated with Eq. (20).

If the activation energy value calculated with intra-particle diffusivity were correct, then according to Weber et al, diffusion is not the only sorption mechanism occurring since it doesn't fall in the typical range for large molecules (12-21 kJ/mol) [50]. This supports similar conclusions made in **Section 4.3** where intra-particle diffusion was not the only mechanism apparent in this system.

Table 8 Activation energy for pseudo-second order rate constant and intra-particle diffusivity for sorption of 4-aminophenol on PEBA as temperature changes.

Temperature (K)	K_2 ($g \cdot mmol^{-1} \cdot min^{-1}$)	D_c x 10^{10} ($m^2 \cdot min^{-1}$)
273	126.2	0.238
283	199.5	0.544
293	266.8	1.01
303	812.9	2.21
313	2566.5	5.26
Activation Energy ($kJ \cdot mol^{-1}$)	52.2	54.0

4.5 Effect of NaCl on Sorption

Kinetic sorption data of 50 ppm and 500 ppm 4-aminophenol on PEBA in the presence of NaCl at different concentrations are shown in **Fig. 26** and **Fig. 27**,respectively.

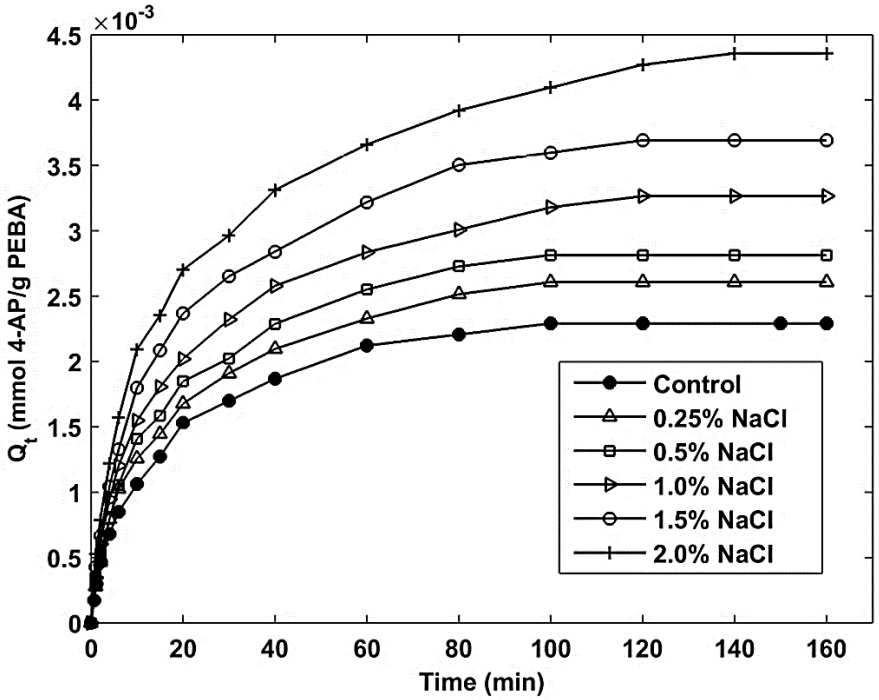

Fig. 26 4-aminophenol uptake on PEBA in the presence of different concentrations of NaCl at 293 K. Control designates 0% NaCl content. Initial concentration of aminophenol 50 ppm.

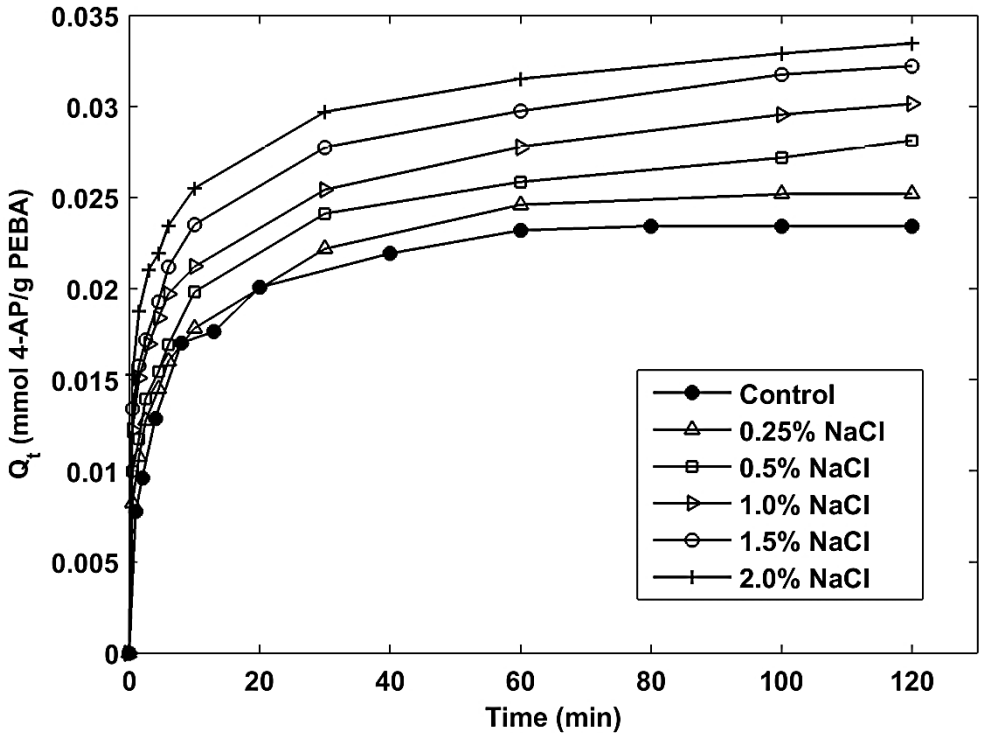

Fig. 27 4-aminophenol uptake over time on PEBA in the presence of different concentrations of NaCl at 293 K. Control designates 0% NaCl content. Initial concentration of aminophenol 500 ppm.

There was a clear increase in the sorption capacity of 4-aminophenol on PEBA as the concentration of NaCl in the feed solution increased. The equilibrium uptake at 50 ppm 4-aminophenol was 2.29×10^{-3} mmol/g with no NaCl present and increases by about twofold to 4.36×10^{-3} mmol/g when NaCl is present at a concentration of 2.0 wt%. A similar scenario was seen with the 500 ppm 4-aminophenol solutions where an equilibrium uptake of 2.58×10^{-2} mmol/g was reached in the absence of NaCl, and it was increased to 3.75×10^{-2} mmol/g when 2.0 wt% of NaCl is present in the solution.

Studies have shown that a presence of salt can have varying effects on sorbate uptake. It can either increase or decrease the sorption uptake depending on the properties of the sorbate/sorbent or the salt concentration. A number of proposed mechanisms exist for this phenomenon including: electrostatic interactions, ion exchange, water adsorption or a salting-out

effect [62]. The most likely reason for this interaction in the 4-aminophenol/PEBA/NaCl system is the salting-out effects due to the relatively low solubility of 4-aminophenol in water. Salting-out results when a high electrolytic content in the solution from dissociated ions (e.g., Na^+ and Cl^-) causes the non-electrolyte (4-aminophenol) to be less soluble in the solvent, increasing its chemical potential and thus can more favourably interact with the sorbent [63]. Electrostatic interactions may also exist in this system between the positive Na^+ ions and either the negative electron donating groups found on the PEBA sorbent or the negative electron donating groups on the 4-aminophenol itself [64][65]. By neutralizing the negatively charged groups on the PEBA, more 4-aminophenol molecules can be sorbed due to the net positive change in surface charge [66]. On the other hand, if the Na^+ can interact directly with 4-aminophenol, it may act as a barrier against negative 4-aminophenol molecules already sorbed to the surface of the PEBA [67]. This barrier could also protect against adjacent 4-aminophenol molecules, to improve stability once sorption occurs [68], although this appears to be unlikely if the mechanism of "co-operative adsorption" is present in this system, as explained during isotherm modelling (**Section 4.1**).

Analysis of the kinetics data with the pseudo-second order (**Fig. 28** and **Fig. 30**) and diffusion (**Fig. 29** and **Fig. 31**) kinetics models resulted in the kinetic parameters shown in **Table 9**.

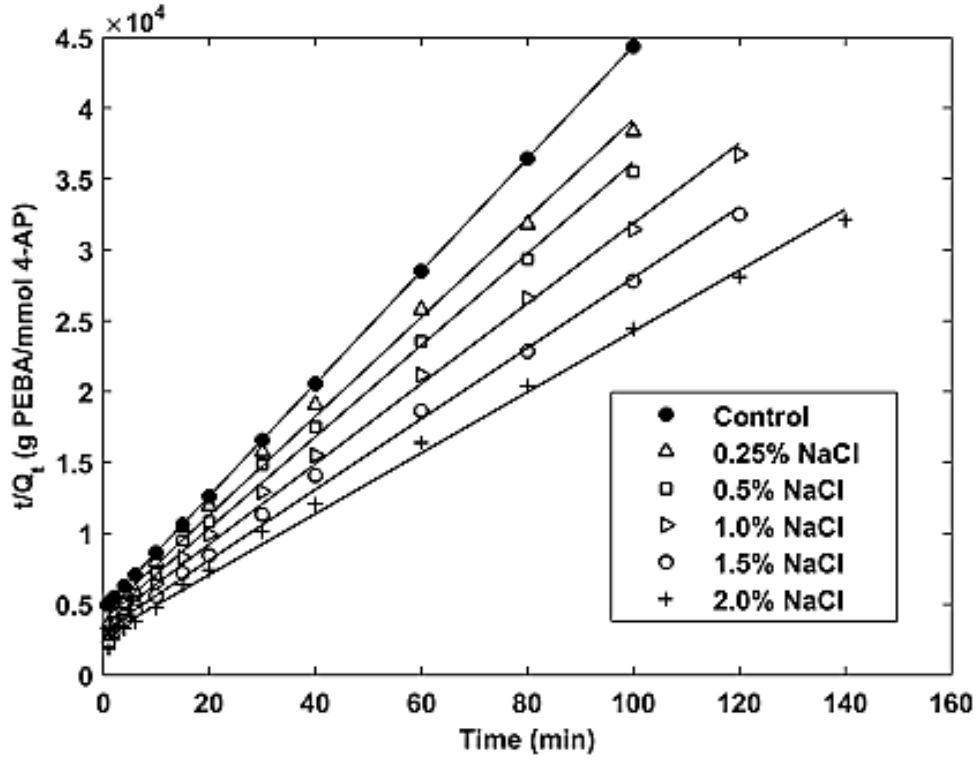

Fig. 28 t/Q_t versus time for sorption of 4-aminophenol (initial concentration 50 ppm) on PEBA in the presence of different concentrations of NaCl.

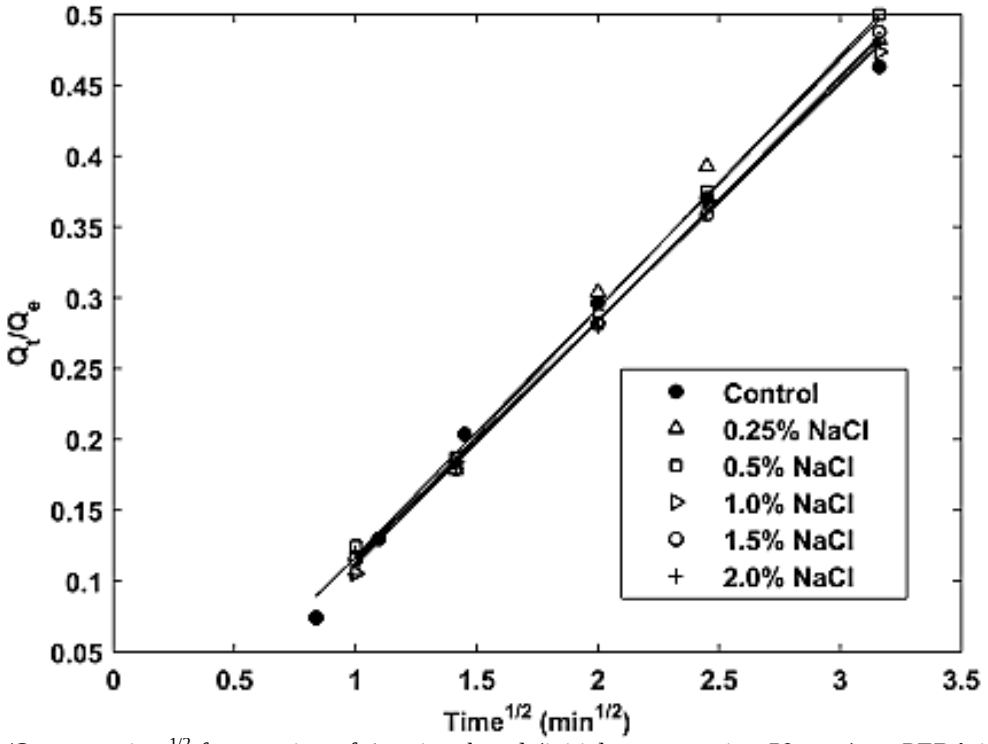

Fig. 29 Q_t/Q_e versus $time^{1/2}$ for sorption of 4-aminophenol (initial concentration 50 ppm) on PEBA in the presence of different concentrations of NaCl.

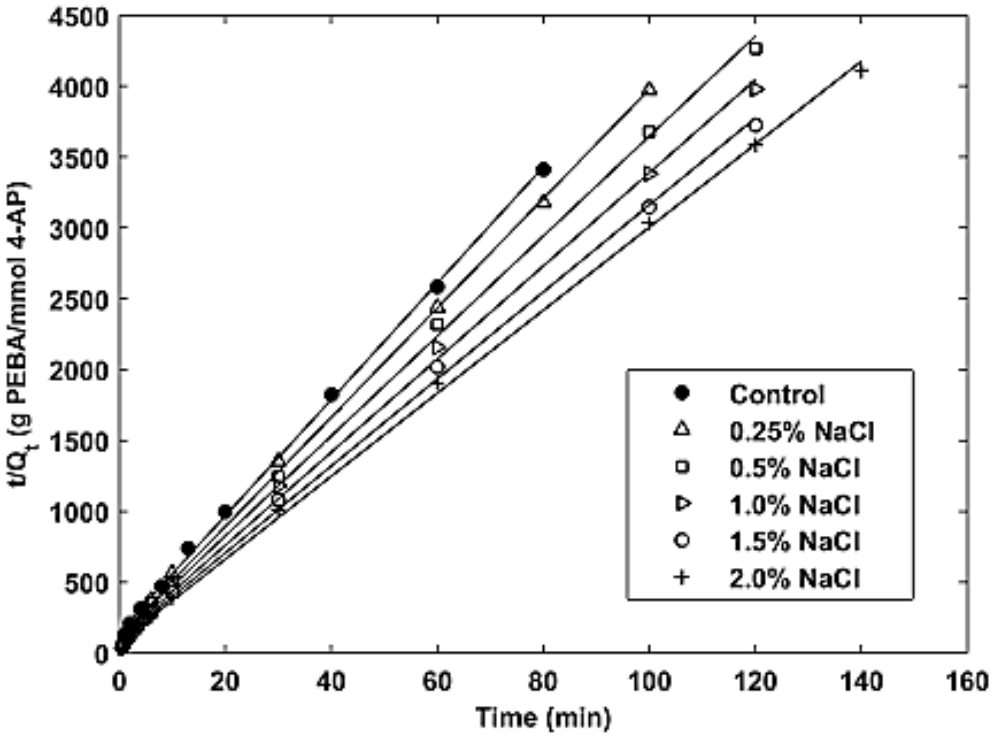

Fig. 30 t/Q_t versus time for sorption of 4-aminophenol (initial concentration 500) ppm on PEBA in the presence of different concentrations of NaCl.

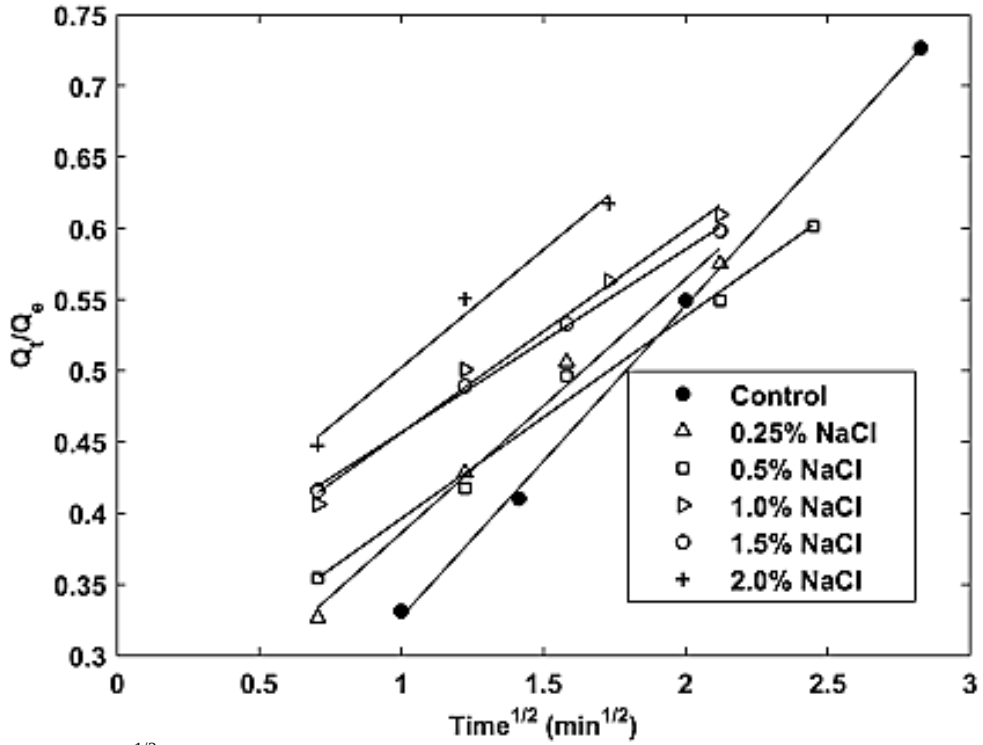

Fig. 31 Q_t/Q_e vs $time^{1/2}$ for sorption of 4-aminophenol (initial concentration500 ppm) on PEBA in the presence of different concentrations of NaCl.

At a 50 ppm 4-aminophenol concentration, increasing the NaCl content caused the second order rate constant to decrease (**Fig. 32**). When the initial 4-aminophenol concentration was increased to 500 ppm, the second order rate constant remained similar for different NaCl concentrations with a mean of about 11.1 g/mmol·min. This means that at low 4-aminophenol concentrations, the rate of sorption is affected by the NaCl content in the solution, but when 4-aminophenol concentrations were high enough the sorption rate dependency of NaCl became less significant.

On the other hand, at 50 ppm 4-aminophenol concentration, the diffusion coefficient remained constant when the NaCl concentration was increased (**Fig. 33**). This indicates that the diffusion rate of aminophenol was not affected by NaCl at low 4-aminophenol concentrations. Once the concentration of 4-aminophenol was increased to 500 ppm, the diffusion coefficient of 4-aminophenol decreased with an increase in the NaCl concentration present in the feed solution. This indicated that 4-aminophenol diffusion was slowed down as more NaCl was present in the system.

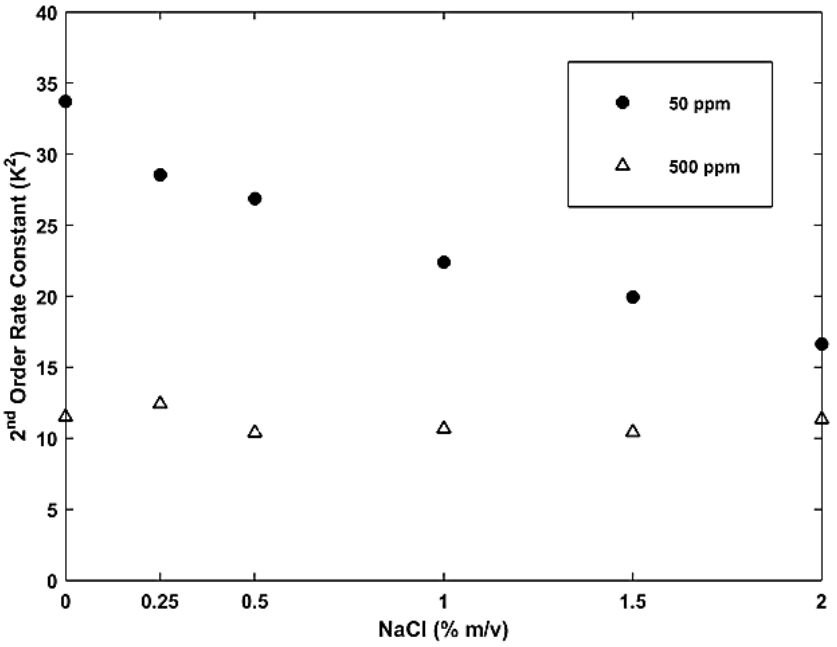

Fig. 32 Second order rate constant (K_2) of 4-aminophenol solutions at 50 and 500 ppm on PEBA versus different NaCl concentrations.

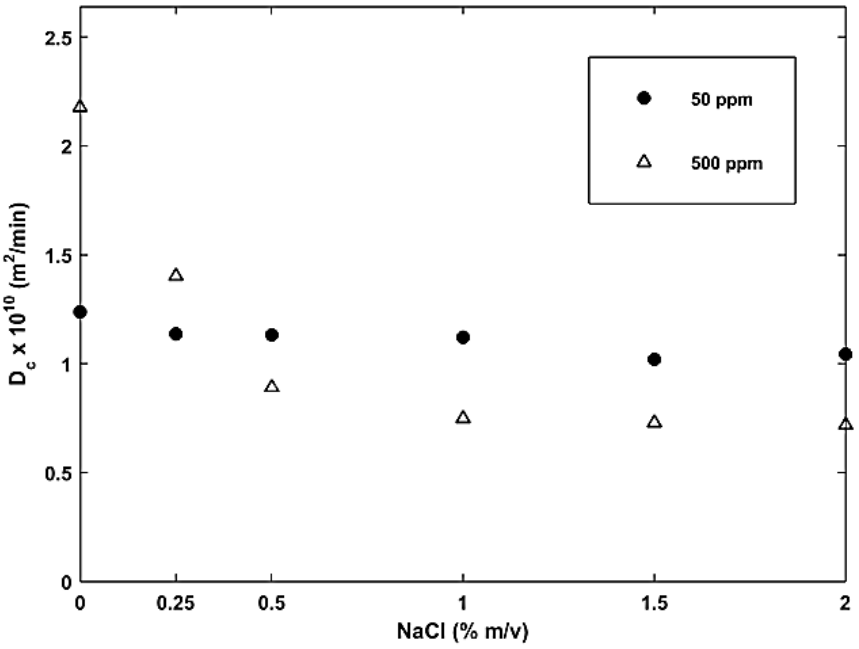

Fig. 33 Diffusion coefficient (D_c) of 4-aminophenol solutions at 50 and 500 ppm on PEBA versus different NaCl concentrations

Table 9 Pseudo-second order rate constants and intra-particle diffusivities for sorption of 4-aminophenol at 50 ppm and 500 ppm on PEBA as NaCl concentration changes.

4-aminophenol Conc.	NaCl Conc. (wt%)	K_2 ($g \cdot mmol^{-1} \cdot min^{-1}$)	D_c x 10^{10} ($m^2 \cdot min^{-1}$)
50 ppm	0.00	33.70	1.238
	0.25	28.53	1.136
	0.50	26.86	1.132
	1.00	22.37	1.121
	1.50	19.93	1.019
	2.00	16.62	1.043
500 ppm	0.00	11.50	2.177
	0.25	12.40	1.401
	0.50	10.37	0.890
	1.00	10.64	0.748
	1.50	10.42	0.728
	2.00	11.32	0.718

4.6 PEBA Sorbent Regeneration

Regeneration of PEBA sorbent after being exposed to 4-aminophenol is highly effective with water, and even more effective with alcohol based regenerative agents such as isopropanol. **Fig. 34** shows the percentage of 4-aminophenol removed from PEBA sorbent after successive sorption runs.

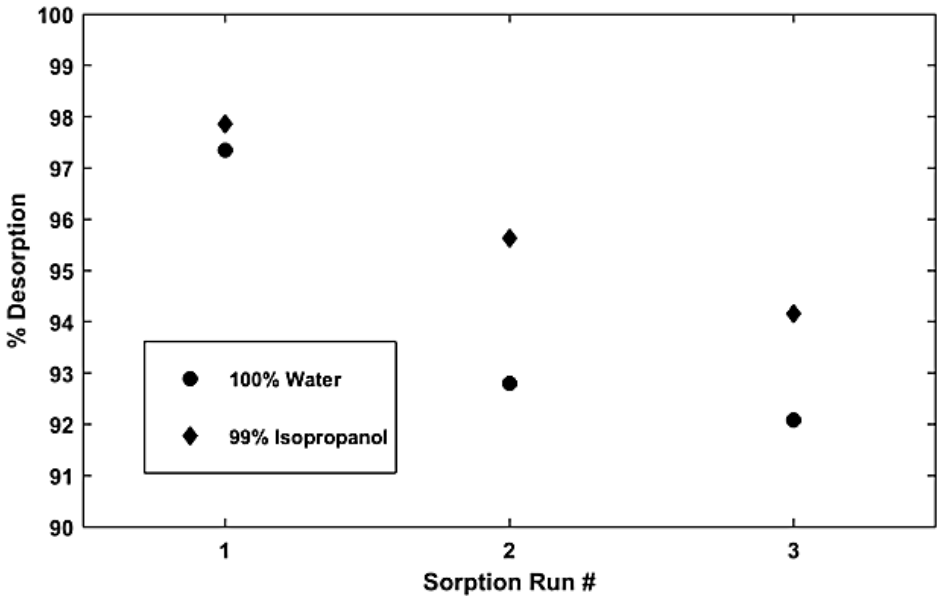

Fig. 34 Desorption of 4-aminophenol in PEBA using water and isopropanol after consecutive sorption/desorption runs.

Since desorption in this study is performed through a batch method, the equilibrium reached between 4-aminophenol in the bulk solution and the 4-aminophenol that was sorbed into the PEBA sorbent dictates the maximum level of 4-aminophenol removal. Thus, it was not possible for desorption to reach 100%, but it does show that desorption with either water or isopropanol was very effective (< 92% after 3 runs) and there is high potential for reuse of the PEBA sorbent. Further investigation into more advanced desorption methods, specifically a thermal desorption technique with a continuous countercurrent flow could offer more effective desorption. Thermal desorption incorporates a temperature change into the desorption procedure and in the case of PEBA and 4-aminophenol it has high potential since the sorption process is effectively exothermic.

Chapter 5

Conclusion and Recommendations

5.1 Conclusions

This study dealt with the sorption of 4-aminophenol from water using poly(ether-block-amide) copolymer (PEBA). A combined Langmuir and Freundlich isotherm model was able to fit the corresponding isotherm data better than with either model alone. In general, the sorption isotherm showed an S3 curve, and the sorption process was found to be exothermic in nature. The sorption followed pseudo-second order kinetics better than pseudo-first order kinetics, and the true rate constants, including the sorption and desorption rate constants, were determined using the Aziniain method. The sorption activation energy for this system was calculated with both pseudo-second order and diffusion kinetic models, and the results further supported that diffusion was not the sole sorption mechanism. When NaCl is present in the system, the sorption uptake capacity increased when NaCl was present at higher concentrations, for which the "salting-out" or electrostatic interactions were likely the reasons. In the presence of NaCl, the pseudo-second order rate constant for 4-aminophenol sorption on PEBA decreased with an increase in NaCl concentration at low 4-aminophenol concentrations, but remained constant when 4-aminophenol concentration was sufficiently high. On the other hand, the diffusion coefficient of 4-aminophenol in PEBA remained constant at lower 4-aminophenol concentrations, and it decreased with an increase in NaCl concentration at higher 4-aminophenol concentrations. Regeneration of the spent PEBA sorbent can be achieved with water and isopropanol.

5.2 Recommendations

Based on the results obtained from this study, the following recommendations for further analysis on the topic of 4-aminophenol sorption with PEBA sorbent can be made:

1. Investigate how other impurities (salts, heavy metals) present in the system could affect 4-aminophenol sorption on PEBA. This would show how robust PEBA sorbent is when other compounds are present.
2. Determine a more appropriate empirical isotherm model for this system to better explain the sorption mechanisms.
3. Determine an alternate kinetics model which can fully explain the sorption mechanisms occurring while ensuring a correct kinetic rate constant.
4. Investigate further into the regeneration and reuse of PEBA sorbent while optimizing for the amount of regenerative agent required. Other methods/modifications for improving regeneration (e.g., different regenerative chemicals, presence of a vacuum or increasing/decreasing temperature) may also be investigated.
5. Further thermodynamic studies aiming to determine the thermodynamic information (including Gibbs free energy, enthalpy and entropy change) of the sorption process to give more insight into the sorption mechanism.

References

[1] W. Kujawski, A. Warszawski, W. Ratajczak, T. Porbski, W. Capała, I. Ostrowska. Application of pervaporation and adsorption to the phenol removal from wastewater. Separation and Purification Technology. 40 (2) (2004) 123-132.

[2] NIIR Board of Consultants & Engineers. (2004). Paracetamol - an analysis of technologies for cleaner production. In NIIR Project Consultancy Services (Ed.), Drugs & pharmaceutical technology handbook (pp. 69-74). Delhi: Asia Pacific Business Press Inc.

[3] V. V. Rakholiya, S. A. Puranik. COD reduction using modifying industrial effluent treatment flowsheet and low cost adsorbent as a part of cleaner production. Advances in Applied Science Research. 3 (3) (2012) 1279.

[4] X. Li, X. Zhou, J. Mu, L. Lu, D. Han, C. Lu, M. Wang. Thermodynamics and kinetics of p-aminophenol adsorption on poly(aryl ether ketone) containing pendant carboxyl groups. Journal of Chemical & Engineering Data. 56 (11) (2011) 4274-4277.

[5] S. Lin, R. Juang. Adsorption of phenol and its derivatives from water using synthetic resins and low-cost natural adsorbents: A review. Journal of Environmental Management. 90 (3) (2009) 1336-1349.

[6] M. K. Mandal, P. K. Bhattacharya. Poly(ether-block-amide) membrane for pervaporative separation of pyridine present in low concentration in aqueous solution. Journal of Membrane Science. 286 (1) (2006) 115-124.

[7] A. Dąbrowski. Adsorption — from theory to practice Advances in Colloid and Interface Science. 93 (1) (2001) 135-224.

[8] Bolis, V. (2013). Fundamentals in adsorption at the solid-gas interface. concepts and thermodynamics. In A. Auroux (Ed.), Calorimetry and thermal methods in catalysis (pp. 3-50). Berlin, Heidelberg: Springer Berlin Heidelberg.

[9] A. Dąbrowski, P. Podkościelny, Z. Hubicki, M. Barczak. Adsorption of phenolic compounds by activated carbon—a critical review. Chemosphere. 58 (8) (2005) 1049-1070.

[10] M. Streat, J. W. Patrick, M. J. C. Perez. Sorption of phenol and para-chlorophenol from water using conventional and novel activated carbons. Water Research. 29 (2) (1995) 467-472.

[11] B. H. Hameed, A. T. M. Din, A. L. Ahmad. Adsorption of methylene blue onto bamboo-based activated carbon: Kinetics and equilibrium studies. Journal of Hazardous Materials. 141 (3) (2007) 819-825.

[12] S. Babel, T. A. Kurniawan. Low-cost adsorbents for heavy metals uptake from contaminated water: A review. Journal of Hazardous Materials. 97 (1) (2003) 219-243.

[13] G. Crini. Non-conventional low-cost adsorbents for dye removal: A review. Bioresource Technology. 97 (9) (2006) 1061-1085.

[14] L. J. Michot, P. J. Thomas. Adsorption of chlorinated phenols from aqueous solution by surfactant-modified pillared clays. Clays and Clay Minerals. 39 (6) (1991) 634-641.

[15] S. Richards, A. Bouazza. Phenol adsorption in organo-modified basaltic clay and bentonite. Applied Clay Science. 37 (1) (2007) 133-142.

[16] U. F. Alkaram, A. A. Mukhlis, A. H. Al-Dujaili. The removal of phenol from aqueous solutions by adsorption using surfactant-modified bentonite and kaolinite. Journal of Hazardous Materials. 169 (1) (2009) 324-332.

[17] R. I. Yousef, B. El-Eswed, A. H. Al-Muhtaseb. Adsorption characteristics of natural zeolites as solid adsorbents for phenol removal from aqueous solutions: Kinetics, mechanism, and thermodynamics studies. Chemical Engineering Journal. 171 (3) (2011) 1143-1149.

[18] B. Okolo, C. Park, M. A. Keane. Interaction of phenol and chlorophenols with activated carbon and synthetic zeolites in aqueous media. Journal of Colloid and Interface Science. 226 (2) (2000) 308-317.

[19] T. Beutel, M. -. Peltre, B. L. Su. Interaction of phenol with NaX zeolite as studied by 1H MAS NMR, 29Si MAS NMR and 29Si CP MAS NMR spectroscopy. Colloids and Surfaces A: Physicochemical and Engineering Aspects. 187 (2001) 319-325.

[20] H. Shu, D. Li, A. A. Scala, Y. H. Ma. Adsorption of small organic pollutants from aqueous streams by aluminosilicate-based microporous materials. Separation and Purification Technology. 11 (1) (1997) 27-36.

[21] M. A. M. Lawrence, R. K. Kukkadapu, S. A. Boyd. Adsorption of phenol and chlorinated phenols from aqueous solution by tetramethylammonium- and tetramethylphosphonium-exchanged montmorillonite. Applied Clay Science. 13 (1) (1998) 13-20.

[22] A. Boulares, M. Tessier, E. Maréchal. Synthesis and characterization of poly(copolyethers-block-polyamides) II. characterization and properties of the multiblock copolymers. Polymer. 41 (10) (2000) 3561-3580.

[23] S. Chhun, B. Saillard, F. MALET, J. ALLANIC. Peba composition and use thereof for manufacturing a transparent object resistant to high-speed impacts. Google Patents. (2013)

[24] J. P. Sheth, J. Xu, G. L. Wilkes. Solid state structure–property behavior of semicrystalline poly(ether-block-amide) PEBAX® thermoplastic elastomers. Polymer. 44 (3) (2003) 743-756.

[25] P. Honore, G. Deleens, E. Marechal. Synthesis and study of various reactive oligomers and of poly(ester-imide-ether)S. European Polymer Journal. 16 (9) (1980) 909-916.

[26] S. Mumcu, K. Burzin, R. Feldmann, R. Feinauer. Copolyetheramides from laurinlactam, decane-1,10-dicarboxylic acid and a,w-dihydroxy-(polytetrahydrofuran). Macromolecular Materials and Engineering. 74 (1) (1978) 49-60.

[27] N. Azizi, M. Arzani, H. R. Mahdavi, T. Mohammadi. Synthesis and characterization of poly(ether-block-amide) copolymers/multi-walled carbon nanotube nanocomposite membranes for CO2/CH4 separation. Korean Journal of Chemical Engineering. (2017)

[28] B. B. Sauer, R. S. McLean, D. J. Brill, D. J. Londono. Morphology and orientation during the deformation of segmented elastomers studied with small-angle X-ray scattering and atomic force microscopy. Journal of Polymer Science Part B: Polymer Physics. 40 (16) (2002) 1727-1740.

[29] S. Armstrong, B. Freeman, A. Hiltner, E. Baer. Gas permeability of melt-processed poly(ether block amide) copolymers and the effects of orientation. Polymer. 53 (6) (2012) 1383-1392.

[30] J. C. Chen, X. Feng, A. Penlidis. Gas permeation through poly(Etherâ€□bâ€□amide) (PEBAX 2533) block copolymer membranes. Separation Science and Technology. 39 (1) (2005) 149-164.

[31] M. Kondo, H. Sato. Treatment of wastewater from phenolic resin process by pervaporation. Desalination. 98 (1) (1994) 147-154.

[32] X. Hao, M. Pritzker, X. Feng. Use of pervaporation for the separation of phenol from dilute aqueous solutions. Journal of Membrane Science. 335 (1) (2009) 96-102.

[33] Y. C. Wong, Y. S. Szeto, W. H. Cheung, G. McKay. Pseudo-first-order kinetic studies of the sorption of acid dyes onto chitosan. Journal of Applied Polymer Science. 92 (3) (2004) 1633-1645.

[34] Y. C. Wong, Y. S. Szeto, W. H. Cheung, G. McKay. Adsorption of acid dyes on chitosan—equilibrium isotherm analyses. Process Biochemistry. 39 (6) (2004) 695-704.

[35] I. Langmuir. The constitution and fundamental properties of solids and liquids. part I. solids. Journal of the American Chemical Society. 38 (11) (1916) 2221-2295.

[36] Tien, C. (1994). *Adsorption calculations and modeling* Boston : Butterworth-Heinemann.

[37] C. Bertagnolli, M. G. C. da Silva, E. Guibal. Chromium biosorption using the residue of alginate extraction from sargassum filipendula. Chemical Engineering Journal. 237 (2014) 362-371.

[38] S. K. Milonjić. A consideration of the correct calculation of thermodynamic parameters of adsorption. Journal of the Serbian Chemical Society. 72 (12) (2007) 1363-1367.

[39] Q. Zhou, W. Gong, C. Xie, D. Yang, X. Ling, X. Yuan, X. Liu. Removal of neutral red from aqueous solution by adsorption on spent cottonseed hull substrate. Journal of Hazardous Materials. 185 (1) (2011) 502-506.

[40] Y. Liu. Is the free energy change of adsorption correctly calculated? Journal of Chemical & Engineering Data. 54 (7) (2009) 1981-1985.

[41] M. M. Haring. Colloid and capillary chemistry (freundlich, herbert). Journal of Chemical Education. 3 (12) (1926) 1454.

[42] J. Simonin. On the comparison of pseudo-first order and pseudo-second order rate laws in the modeling of adsorption kinetics. Chemical Engineering Journal. 300 (2016) 254-263.

[43] S. Lagergren. About the theory of so-called adsorption of soluble substances. Kungliga Svenska Vetenskapsakademies Handlingar. 24 (4) (1898) 1-39.

[44] Y. Ho. Review of second-order models for adsorption systems. Journal of Hazardous Materials. 136 (3) (2006) 681-689.

[45] G. Blanchard, M. Maunaye, G. Martin. Removal of heavy metals from waters by means of natural zeolites. Water Research. 18 (12) (1984) 1501-1507.

[46] T. Gosset, J. Trancart, D. R. Thévenot. Batch metal removal by peat. kinetics and thermodynamics. Water Research. 20 (1) (1986) 21-26.

[47] Y. S. Ho, G. McKay. Pseudo-second order model for sorption processes. Process Biochemistry. 34 (5) (1999) 451-465.

[48] Y. S. Ho, G. Mckay. The kinetics of sorption of basic dyes from aqueous solution by sphagnum moss peat. Canadian Journal of Chemical Engineering. 76 (4) (1998) 822-827.

[49] F. Wu, R. Tseng, R. Juang. Initial behavior of intraparticle diffusion model used in the description of adsorption kinetics. Chemical Engineering Journal. 153 (1) (2009) 1-8.

[50] Morris, C. J., & Weber, W. J. (1964). Removal of biologically resistant pollutant from waste water by adsorption. In B. A. Southgate (Ed.), Advances in water pollution research (pp. 231-266). Pergamon.

[51] Ruthven, D. M. (1984). Principles of adsorption and adsorption processes. Wiley.

[52] V. Ragaini, R. Fois, V. M. Le, M. G. Cattania. A simplified calculation method to evaluate intraparticle diffusivity from sorption kinetic measurements. application of the diffusion of xylenes in 13X and ZSM zeolites. The Canadian Journal of Chemical Engineering. 62 (5) (1984) 706-712.

[53] K. C. Brown, J. F. Corbett. Benzoquinone imines. part 16. oxidation of p-aminophenol in aqueous solution. Journal of the Chemical Society. (3) (1979) 308-311.

[54] C. H. Giles, T. H. MacEwan, S. N. Nakhwa, D. Smith. Studies in adsorption. part XI. A system of classification of solution adsorption isotherms, and its use in diagnosis of adsorption mechanisms and in measurement of specific surface areas of solids. Journal of the Chemical Society. (1960) 3973-3993.

[55] Y. S. Ho, G. McKay. A kinetic study of dye sorption by biosorbent waste product pith. Resources, Conservation and Recycling. 25 (3) (1999) 171-193.

[56] Y. S. Ho, G. Mckay. Kinetic models for the sorption of dye from aqueous solution by wood. Process Safety and Environmental Protection. 76 (2) (1998) 183-191.

[57] Y. S. Ho, G. McKay. The kinetics of sorption of divalent metal ions onto sphagnum moss peat. Water Research. 34 (3) (2000) 735-742.

[58] Y. S. Ho, G. McKay. Sorption of dye from aqueous solution by peat. Chemical Engineering Journal. 70 (2) (1998) 115-124.

[59] S. Azizian. Kinetic models of sorption: A theoretical analysis. Journal of Colloid and Interface Science. 276 (1) (2004) 47-52.

[60] H. Qiu, L. Lv, B. Pan, Q. Zhang, W. Zhang, Q. Zhang. Critical review in adsorption kinetic models. Journal of Zhejiang University-SCIENCE A. 10 (5) (2009) 716-724.

[61] S. Yang, B. Yan, J. Wu, L. Lu, K. Zeng. Temperature-dependent lithium-ion diffusion and activation energy of Li1.2Co0.13Ni0.13Mn0.54O2 thin-film cathode at nanoscale by using electrochemical strain microscopy. ACS Applied Materials & Interfaces. 9 (16) (2017) 13999-14005.

[62] H. A. Arafat, M. Franz, N. G. Pinto. Effect of salt on the mechanism of adsorption of aromatics on activated carbon. Langmuir. 15 (18) (1999) 5997-6003.

[63] A. Kalra, N. Tugcu, S. M. Cramer, S. Garde. Salting-in and salting-out of hydrophobic solutes in aqueous salt solutions. The Journal of Physical Chemistry B. 105 (27) (2001) 6380-6386.

[64] P. Lafrance, M. Mazet. Adsorption of humic substances in the presence of sodium salts. Journal - American Water Works Association. 81 (4) (1989) 155.

[65] G. McKay. Adsorption of dyestuffs from aqueous solutions with activated carbon I: Equilibrium and batch contact-time studies. Journal of Chemical Technology and Biotechnology. 32 (7-12) (1982) 759-772.

[66] M. Mazet, A. Yaacoubi, P. Lafrance. Influence des ions metalliques liberes par un charbon actif sur l'adsorption de micropolluants organiques. le role des ions calcium. Water Research. 22 (10) (1988) 1321-1329.

[67] A. Gundogdu, C. Duran, H. B. Senturk, M. Soylak, D. Ozdes, H. Serencam, M. Imamoglu. Adsorption of phenol from aqueous solution on a low-cost activated carbon produced from tea industry waste: Equilibrium, kinetic, and thermodynamic study. Journal of Chemical & Engineering Data. 57 (10) (2012) 2733-2743.

[68] V. L. Snoeyink, W. J. Weber, H. B. Mark. Sorption of phenol and nitrophenol by active carbon. Environmental Science & Technology. 3 (10) (1969) 918-926.

Appendix

Appendix I – Supporting Figures

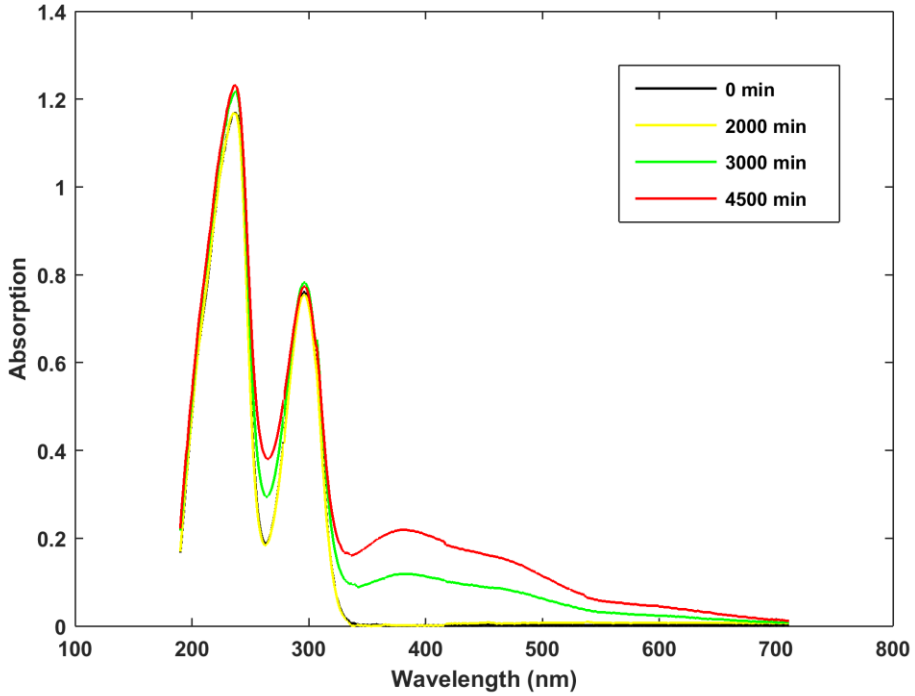

Fig. A. 1 UV/Vis absorption spectrum for 50 ppm 4-aminophenol solution at 273 K over time span of 0 – 4500 min.

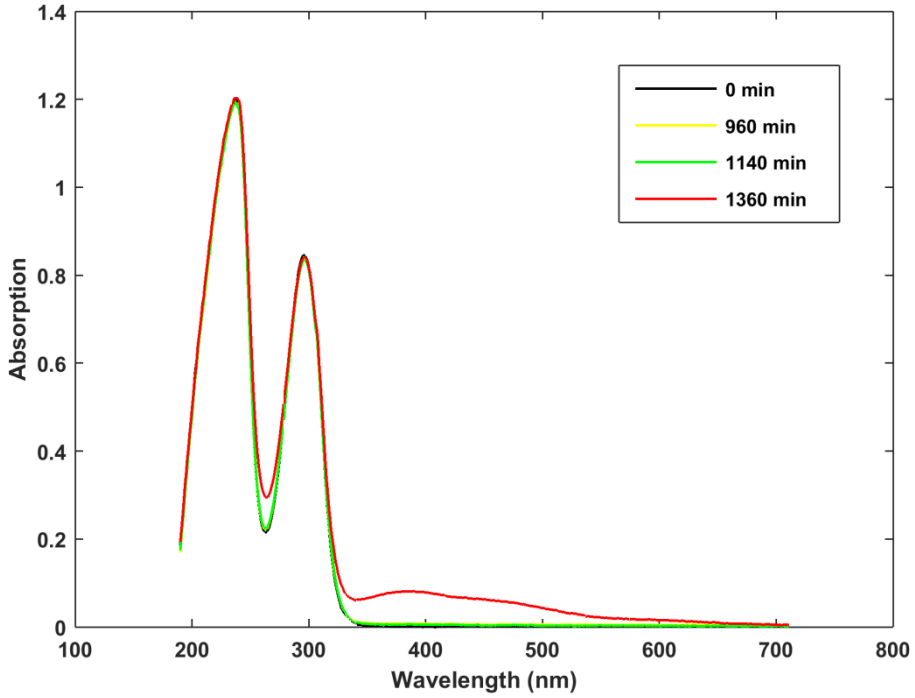

Fig. A. 2 UV/Vis absorption spectrum for 50 ppm 4-aminophenol solution at 283 K over time span of 0 – 1360 min.

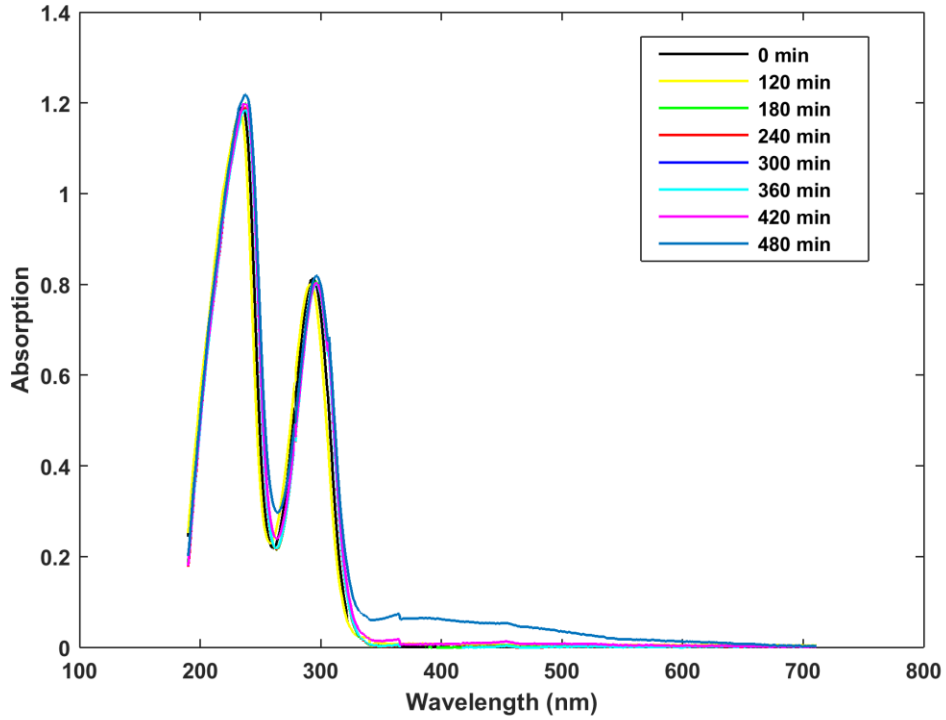

Fig. A. 3 UV/Vis absorption spectrum for 50 ppm 4-aminophenol solution at 293 K over time span of 0 – 480 min.

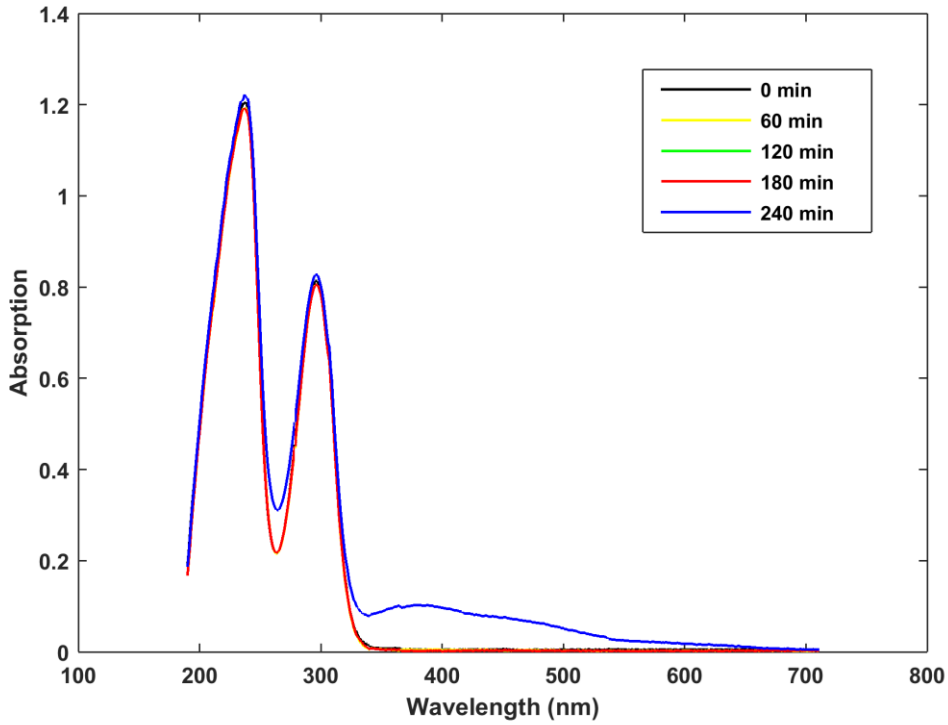

Fig. A. 4 UV/Vis absorption spectrum for 50 ppm 4-aminophenol solution at 298 K over time span of 0 – 240 min.

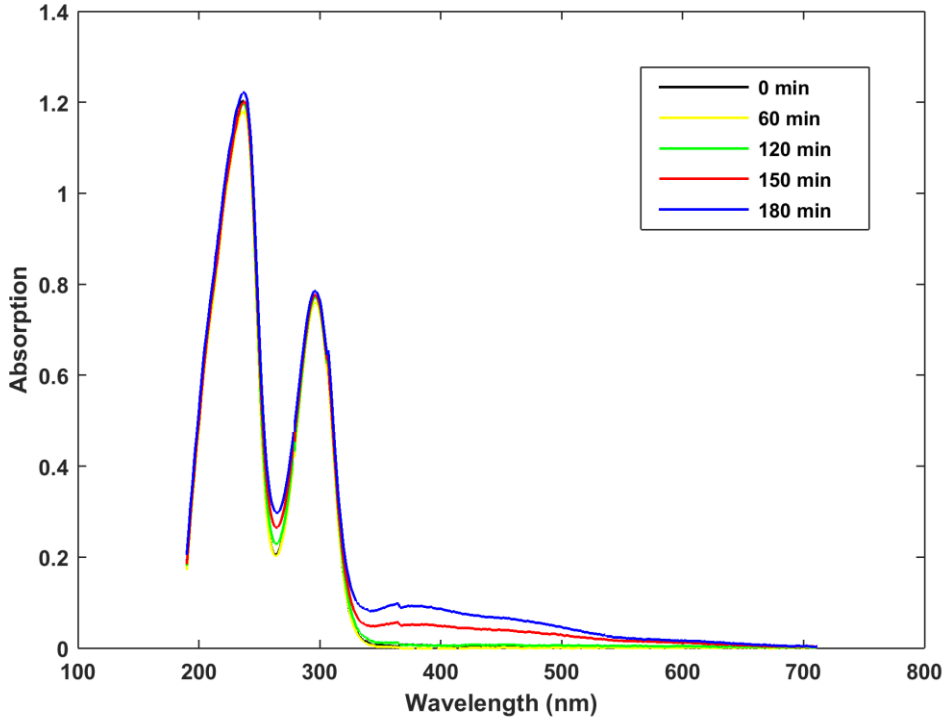

Fig. A. 5 UV/Vis absorption spectrum for 50 ppm 4-aminophenol solution at 303 K over time span of 0 – 180 min.

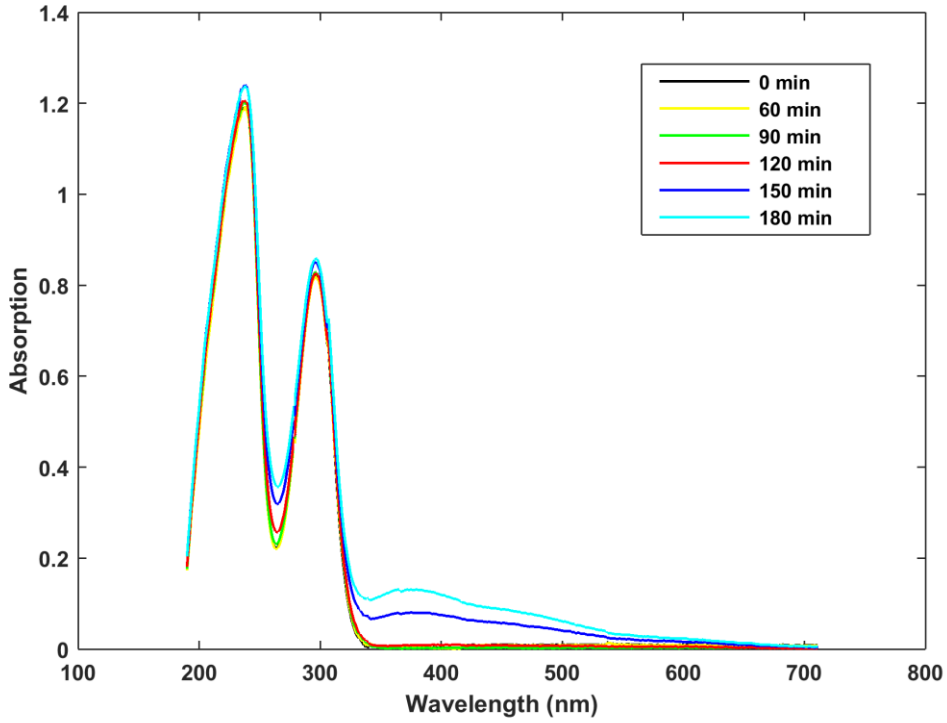

Fig. A. 6 UV/Vis absorption spectrum for 50 ppm 4-aminophenol solution at 308 K over time span of 0 – 180 min.

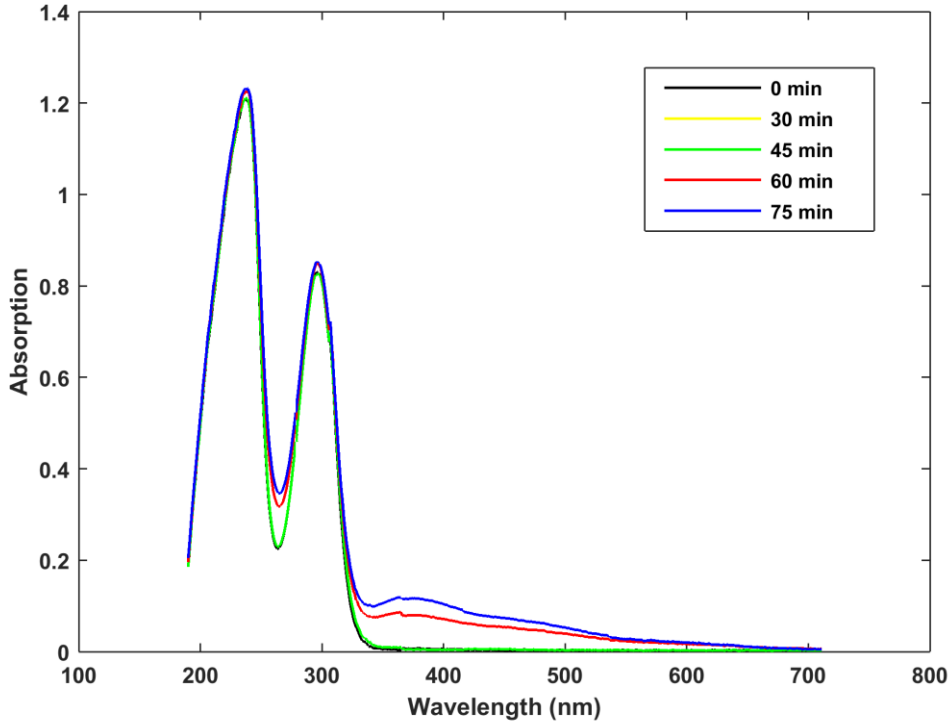

Fig. A. 7 UV/Vis absorption spectrum for 50 ppm 4-aminophenol solution at 313 K over time span of 0 – 75 min.

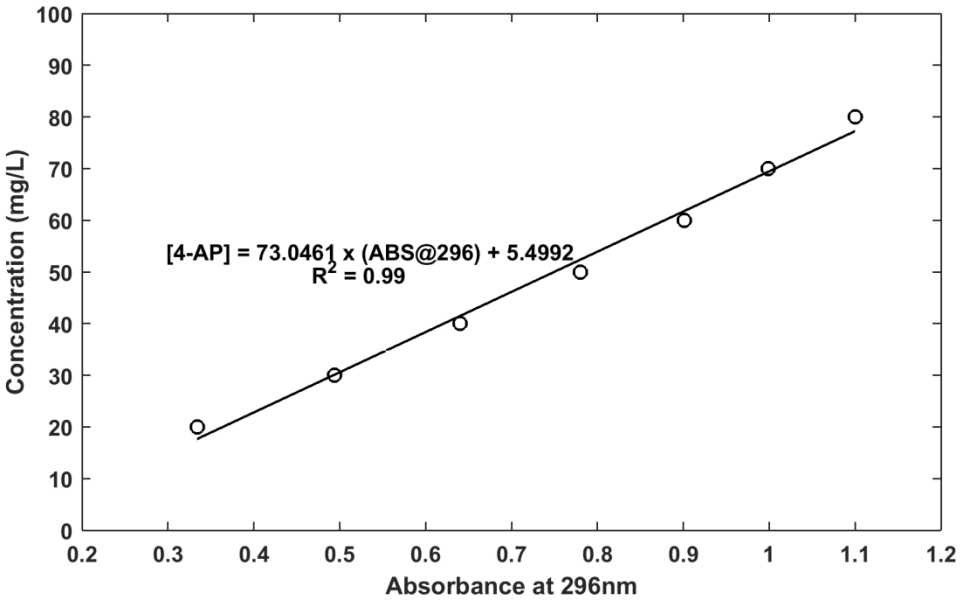

Fig. A. 8 UV-Vis Spectrophotometer calibration curve for aqueous 4-aminophenol from 20 – 80 ppm.

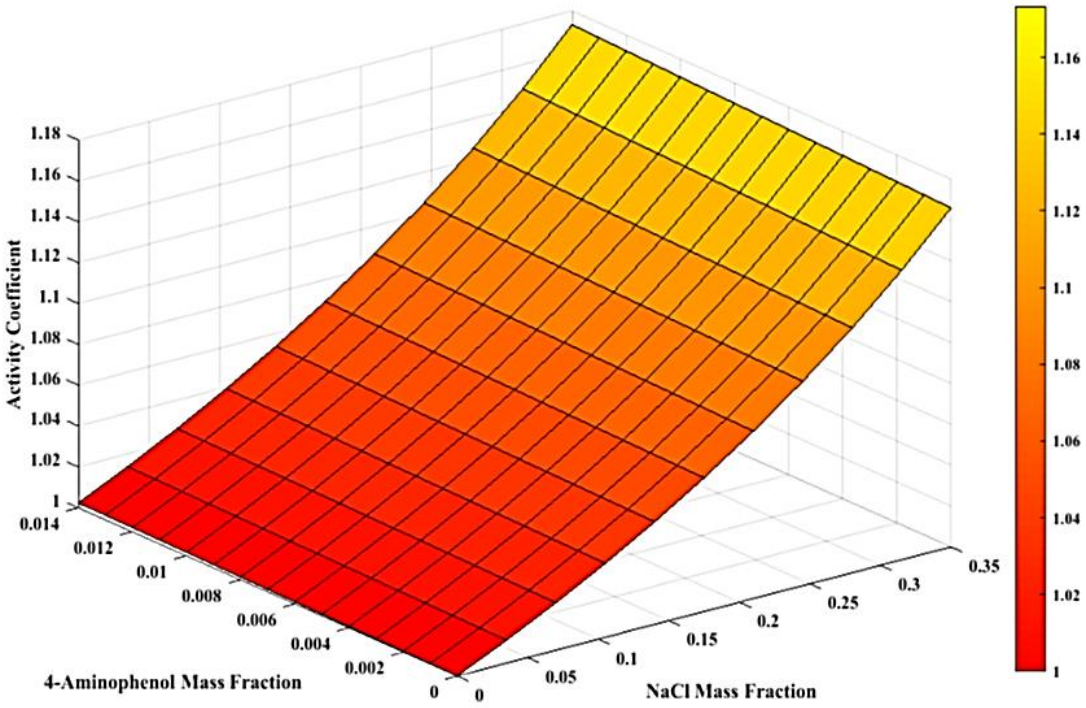

Fig. A. 9 Activity coefficient of 4-aminophenol in water as 4-aminophenol and NaCl mass fractions change.